PREPERATION AND CHARACTERIZATION OF CARBON SUPPORTED PLATINUM NANOPARTICLES FOR METHANOL OXIDATION REACTIONS

A THESIS SUBMITTED TO
THE GRADUATE SCHOOL OF NATURAL AND APPLIED SCIENCES
OF
MIDDLE EAST TECHNICAL UNIVERSITY

BY

AYSU ÇOKANGIN

IN PARTIAL FULFILLMENT OF THE REQUIREMENTS
FOR
THE DEGREE OF MASTER OF SCIENCE
IN
CHEMISTRY

APRIL 2015

Approval of the thesis:

PREPERATION AND CHARACTERIZATION OF CARBON SUPPORTED PLATINUM NANOPARTICLES FOR METHANOL OXIDATION REACTIONS

submitted by **AYSU ÇOKANGIN** in partial fulfillment of the requirements for the degree of **Master of Science in Chemistry Department, Middle East Technical University** by,

Prof. Dr. Gülbin Dural Ünver
Dean, Graduate School of **Natural and Applied Sciences** _____

Prof. Dr. İlker Özkan
Head of Department, **Chemistry** _____

Prof. Dr. Gülsün Gökağaç
Supervisor, **Chemistry Department, METU** _____

Examining Committee Members:

Prof. Dr. Gülsün Gökağaç
Chemistry Dept., METU _____

Prof. Dr. Ceyhan Kayran
Chemistry Dept., METU _____

Assoc. Prof. Dr. Ayşen Yılmaz
Chemistry Dept., METU _____

Assoc. Prof. Dr. Metin Aydin
Chemistry Dept.,Ondokuz Mayıs University _____

Assoc. Prof. Dr. Emren Nalbant Esentürk
Chemistry Dept., METU _____

Date: April 28, 2015

I hereby declare that all information in this document has been obtained and presented in accordance with academic rules and ethical conduct. I also declare that, as required by these rules and conduct, I have fully cited and referenced all materials and results that are not original to this work.

Name, Last name: Aysu ÇOKANGIN

ABSTRACT

PREPERATION AND CHARACTERIZATION OF CARBON SUPPORTED PLATINUM NANOPARTICLES FOR METHANOL OXIDATION REACTIONS

Çokangın, Aysu

M. Sc., Department of Chemistry

Supervisor: Prof. Dr. Gülsün Gökağaç

April 2015, 64 pages

In this thesis, carbon supported platinum nanoparticle catalysts were synthesized by using $PtCl_4$ as precursor, sodium borohydride (Cat I), hydrazinum hydroxide (Cat II) and formaldehyde (Cat III) as reducing agent and 1-heptanamine (a), N-methylheptanamine (b) and N,N-dimethylheptanamine (c) as surfactants for methanol oxidation reaction. Their physical and electrochemical properties were determined by inductively coupled plasma spectroscopy (ICP), cyclic voltammetry (CV), and characterization methods of X-ray diffraction (XRD), X-photoelectron Spectroscopy (XPS), transmission electron microscopy (TEM) and Brunauer, Emmnett and Teller (BET) surface area analysis.

XRD and TEM results indicated that all catalysts exhibit face centered cubic structure and contain small and agglomerated platinum particles in different shape, size, ratio and density. Cat I composed of small (~ 5 nm) and significant number of quite dense spherical agglomerated (~ 20 - ~ 150 nm) particles, Cat II comprises small (~ 5 nm) cubic and formless agglomerated (~ 20 - ~ 300 nm) particles and Cat

III contains large number of small (~ 5 nm) and a few number of spherical, less dense and agglomerated (~ 20 - ~ 200 nm) particles.

XPS data displayed that platinum exist in two different oxidation states, Pt(0) (~64.5-~69.6 %) and Pt(IV) (~35.5-~30.4 %) and platinum surface includes adsorbed OH, H_2O, C-O, C=O, C-OH, partially crystalline carbon and/or hydrocarbon.

BET analysis showed that the surface area of the Cat Ia, IIa, IIIa, Ib, IIb, IIIb, Ic, IIc and IIIc are 27.58, 27.88, 36.25, 5.44, 6.27, 6.22, 26.80, 32.50 and 52.88 m^2/ g Pt respectively. The highest surface area recorded to catalyst IIIc. These results illustrated that surface area of the catalyst depends on the reducing agent that was used. However no trace was found to indicate the surfactant effect on the surface area of catalysts.

Electrochemical studies revealed that the order of performance of catalysts towards methanol oxidation reaction is Catt II < Cat I < Cat III and Cat IIIc has the highest performance, which is 2.23 times larger than E-TEK catalyst. It was found that the performance of catalysts depends on the kind of surfactant and reducing agent, electrochemical surface area, percent platinum utility, roughness factor, and If / Ir ratio.

Keywords: Direct Methanol Fuel Cells, Carbon Supported Platinum Catalysts, Cyclic Voltammeter, Transmission Electron Microscopy, X-ray Diffraction, X-ray Photoelectron Spectroscopy.

ÖZ

KARBON DESTEKLİ PLATİN KATALİZÖRLERİN HAZIRLANMASI, KARAKTERİZASYONU VE METHANOL YÜKSELTGENME REAKSİYONUNDAKİ PERFORMANSI

ÇOKANGIN, Aysu
Yüksek Lisans, Kimya Bölümü
Tez Yöneticisi: Prof. Dr. Gülsün Gökağaç

Nisan 2015, 64 sayfa

Bu tezde, başlangıç maddesi olarak $PtCl_4$, indirgeyici olarak sodyum borohidrit (Kat I), hidrazin (Kat II) ve formaldehit (Kat III)) ve sürfaktan heptanamin, N,metilheptanamin, N,N-dimetilheptanamin kullanılarak metanol yükseltgenme tepkimesi için karbon destekli platin nanoparçacıklar içeren katalizörler sentezlenmiştir. Hazırlanan katalizörlerin fiziksel ve elektrokimyasal özellikleri, eşleşmiş plazma (ICP), dönüşümlü voltametre (CV), X-ışınları kırınımı (XRD), X-ışınları fotoelektron spektroskopisi (XPS), transmisyon (geçirmeli) elektron mikroskopu (TEM) ve Brunauer, Emmnett and Teller (BET) yüzey analizi teknikleri kullanılarak tayin edilmiştir.

XRD ve TEM sonuçlarına göre, bütün katalizörlerin yüzey merkezli küp kristal yapısına sahip olduğu gözlemlenmiştir. Ayrıca bu sonuçlar bütün katalizörlerin küçük ve değişik şekil, büyüklük, oran ve yoğunlukta olduğunu göstermektedir. Kat I küçük (~ 5 nm) küp şeklinde ve şekilsiz büyük (~ 20 - ~ 150 nm) parçacıklardan, Kat II küçük (~ 5 nm) ve önemli miktarda yoğun, yuvarlak büyük (~ 20 - ~ 300 nm)

parçacıklardan, Kat III ise küçük (~ 5 nm) ve daha az sayıda , yuvarlak, az yoğun büyük (~ 20 - ~ 200 nm) parçacıklardan oluştuğunu göstermektedir.

XPS verileri, platinin iki farkli yükseltgenme basamağınan oluştuğunu, Pt(0) (~64.5-~69.6 %) ve Pt(IV) (~35.5-~30.4 %), platin yüzeyinin OH, H_2O, C-O, C=O, C-OH ile kaplandığını göstermektedir.

BET yüzey analizi sonuçlarına göre, katalizörlerin yüzey alanları Ia, IIa, IIIa, Ib, IIb, IIIb, Ic, IIc ve IIIc için sırasıyla 27.58, 27.88, 36.25, 5.44, 6.27, 6.22, 26.80, 32.50 ve 52.88 m^2/g Pt dir. En geniş yüzeye sahip katalizörün IIIc olduğu görülmektedir. Elde edilen veriler doğrultusunda, katalizörün yüzey alanının indirgeyici etkisiyle değişirken, sürfaktandan bağımsız olduğu anlaşılmıştır.

Elektrokimyasal çalışmalar, hazırlana katalizörlerin metanol yükseltgenme tepkimesine karşı performanslarının Kat II < Kat I < Kat III şeklinde olduğunu göstermiştir. En aktif katalizör Kat IIIc olarak bulunmuştur, bu değer E-TEK 2.23 kat daha fazladır.

Katalizörlerin performanslarının sürfaktan ve indirgeyicilerin çeşidine, elektrokimyasal yüzey alanına, platin kullanılma yüzdesine, pürüzlülük faktörüne ve If / Ir oranına bağlı olduğu bulunmuştur..

Keywords: Doğrudan Metanol Yakıt Hücreleri, Karbon Destekli Platin Katalizörleri, Çevrimsel Voltametre, Geçirimli Elektron Mikroskobu, X-ısınları Kırınımı Spektrometresi ve X-ısınları Fotoelektron Spektrometresi.

To my mum….

ACKNOWLEDGEMENTS

I would like to express my deepest appreciation and thanks to my advisor Prof. Dr. Gülsün Gökağaç for her warm-hearted support, aspiring attention, enlightening guidance, understanding, invaluably constructive criticism and infinite patiance. It was a big privilege to work with her and take advantage of her wide knowledge store. Her tremendous mentor have been of great value for me. Her advice on both research as well as on my career have been priceless.

I offer my special gratitude to Sevda Kalyoncu for her friendship and the endless encourage which she gave me. I gratefully thank to lab partners Deniz Cakal and Seda Ergan for their support, motivation and friendship during my studies.

I owe many thanks to my precious friends Zeki Sahin and Melike Caglayan who are the only people in world believe in me definitely just for being myself. Their existance whenever I needed, is treasure to me.

I also would like to thank to TUBITAK for the financial support (Project No. 111T162) and to METU Central Laboratory for the analysis.

I cannot express enough thanks to my family who always loved me. Especially a special thanks to my mum who incents me to strive towards my goal and indulge me always with her endless and unconditional love. Without her immeasurable sacrifice, I can never succeed.

At the end I would like express my deepest appreciation to Mustafa Çokangın who always supports me and shows me that love changes everything.

TABLE OF CONTENTS

LIST OF TABLES

TABLES

LIST OF FIGURES

FIGURES

CHAPTER 1

INTRODUCTION

1.1. FUEL CELLS

A fuel cell is an electrochemical device which directly converts the chemical energy into electricity with high conversion yield and generally combine fuel and oxidant to operate. They consist of an anode (a negative electrode), a cathode (a positive electrode), catalysts, an intervening electrolyte, and an attached electrical circuit.

Each cell contains an electrolyte located between two electrodes. The electrodes are commonly accompanied by catalysts, which include metals. Fuel is continuously fed to the anode part to be oxidized and oxidant is continuously fed to the cathode part to be reduced to water. Schematic representation of a fuel cell can be seen in Figure1.1.

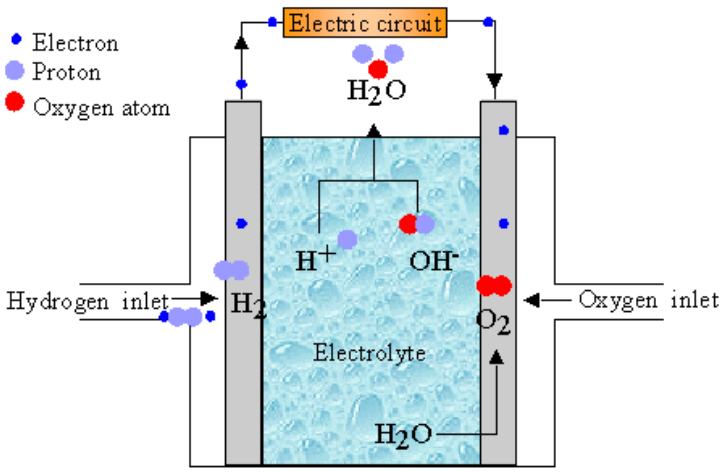

Figure 1.1. Schematic representation of a fuel cell.

Fuel cell is a battery like device but continuous. They do not require recharging the same as a battery. In theory they may produce energy as long as fuel is constantly supplied without any self-discharge occurs.

There are many advantages such as:

- Fuel cells are called green energy systems which eliminate pollution resulting from burning fossil fuels.
- Greenhouse gases are mostly prevented since the hydrogen source can be supplied by electrolysis of water
- No conventional fuels are necessary, therefore economical dependence on foreign countries can be eliminated.
- Fuel cells have a higher efficiency per volume than other devices.
- They have consistency to changing electrical loads.
- They operates silently.
- They are ideal for military applications, since low heat transmission for low temperature fuel cells.
- Fuel cells can provide high quality DC power.

Beside the glorious properties of fuel cells, some disadvantages also exist and the system needs to be enhanced in future progress such:

- For some fuel cells, transportation and storage problems exist.
- Fuel cells have manufacturing cost and very expensive systems.
- They have long operating times compared with other devices.

Fuel cells are versatile and may use various applications as transportation, distributed power generation, structures, accessory uses, military, space and defense applications, electric vehicles[81] and electronic portable devices.

1.2. SIGNIFICANCE OF FUEL CELLS

It is well known that the energy sources in the world are insufficient because of an increase in energy demand. The increasing demand for energy and deficiency of energy sources lead the researchers to find out alternative methods. One of the biggest developments in electrochemistry of the last decades is the conversion of chemical energy into electrical energy via fuel cells. Whereas the 19^{th} Century was the century of the steam engine and the 20^{th} Century was the century of the internal combustion engine, it is likely that the 21^{st} Century will be the century of the fuel cell. Fuel cells are developing technology as clean energy production devices that are popular for researchers and it is believed that it will play an important role on energy industry in future which required avoiding future problems of oil depletion and global warming due to burning of fossil fuels.

1.3. THE HISTORY OF FUEL CELLS

In 1791 Italian physiologist Luigi Galvani's who was the first person opened the door of electrochemical power sources, gained a new perspective by remarkable experiments among muscles of dead frogs legs. In 1792, Alessandro Volta, an Italian physicist developed to this phenomenon by demonstrating the generation of a galvanic effect between two metals. In the light of this phenomenon, in March 1800, Volta concluded a new device which is known as Volta pile that could result in continuously provided electrical current to a circuit. Since this was the first electrochemical power source, very important for the science of electrochemistry. Then properties of the electric current and electrochemical processes were discovered.

In May 1802, William Nicholson and Sir Anthony Carlisle performed the hydrogen and oxygen production with electrolysis of water. In the 1830s, British Sir William Robert Grove, conducted a series of experiments related to water electrolysis. He designed the device which is given in Figure 1.3 by dipping two platinum electrodes into solution of sulfuric acid. He carried out the reverse reaction to produce energy and observed evolution of gases hydrogen and oxygen after disconnecting the current and seems that the polarization of electrodes occurred which shows the durability of potential difference between electrodes. Combining those electrodes with an external circuit, flow of current was observed and *gas voltaic battery* was invented. By this invention, in February 1839, Grove's experiments were figured in the *Philosophical Magazine* by announcing the first fuel cell prototype.

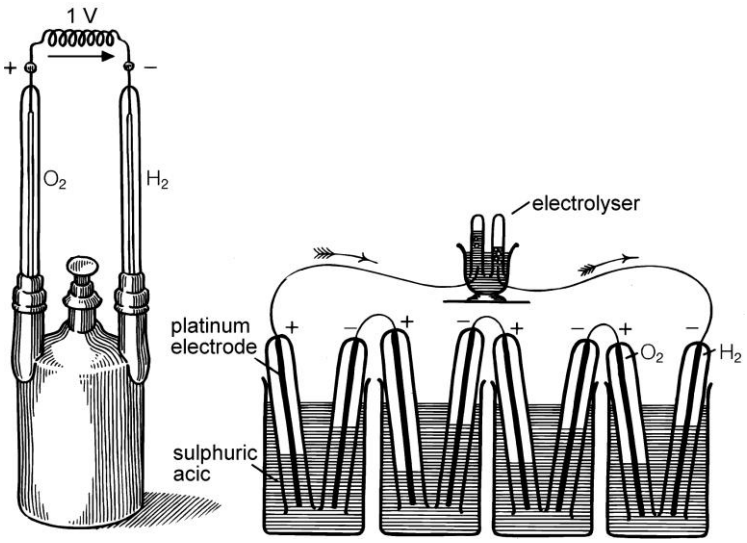

Figure 1.2. Grove's 'gas battery' (1839).

In 1882, Lord Rayleigh developed a new gas battery prototype to enhance the efficiency of the platinum electrode by the increase of surface action between the solid electrode, the liquid and the gas. Rayleigh was the person who first used coal as source and surprisingly obtained notably current when compared the inferior quality of the source used.

In 1889, Ludwig Mond and Carl Langer presented a new form of gas battery. In this form, sulfuric acid was used for matrix formation to prevent the electrode flooding problem. For carrying the fuel cell reaction, Mond and Langer used on air and industrial coal gas. Their aim was to increase the surface of the catalyst. For this purpose, they built a fuel cell which is very similar to the modern day technology.

In 1894, Wilhelm Ostwalt (Nobel Prize owner, 1909), an architect of the physical chemistry, experimentally determined the functions of fuel cell components which are electrodes, electrolyte, oxidizing and reducing agents, anions, and cations. He also considered the electrochemistry as a solution to avoid the low yield energy conversion of steam engine. He proposed that high amount of heat was used to burn

the coal in order to convert the chemical energy to electrochemical energy. By using electrochemistry than steam engine provides higher energy conversion yield, whereas heat loss will be prevented.

In 1896, William Jacques constructed the first galvanic cells by producing electricity directly from coal. Thus, "carbon battery" was constructed in which air was injected into an alkali electrolyte to react with a carbon electrode shown in Figure 1.4.

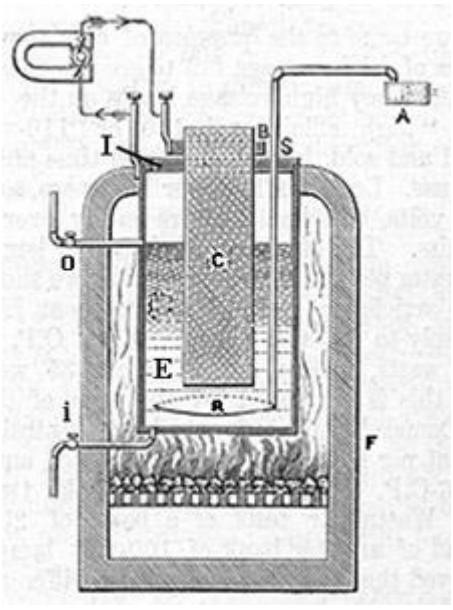

Figure 1.3. William Jacques' carbon cell, 1896 (digitally enhanced)

Haber and Bruner were the first scientists who concluded the electrochemical reaction between the coal and electrolyte in molten alkaline in 1904 by achieving the indirect oxidation of coal. After several experiments, in 1912, Baur and Ehrenberg found out a suitable electrolyte using hydroxide, carbonate, silicate and borate and with molten silver as cathode.

In 1930s the Armenian scientist Oganes Davtyan also developed an electrolyte which consists of several compounds to obtain an electrode with high conductivity and

stability. He conducted several experiment with high and low temperature fuel cells. He operated a fuel cell which can oxidized CO with oxygen in the air at 700 °C. He published the book "The Problem of Direct Conversion of the Chemical Energy of Fuels into Electrical Energy" in 1947 which containing all his studies about the problem of fuel cells. This book had placed in history as the first book in the world about fuel cells.

Francis Thomas Bacon in 1932, studied with alkaline fuel cells. He performed the fuel cell experiments with activated nickel electrodes and alkaline electrolyte (KOH) instead of using acid solutions, since the acid solution would cause corruption. Bacon used porous, gas-diffusion electrodes in order to keep gases away. Patent of this design was taken out as *Bacon cell* in 1959 by working on a project to provide electrical power for Apollo.

Between the years 1935 and 1937, Baur and Brunner searched for the enhancement of the fuel cell efficiency by addition of CO_2 to cathode. They focused on ceramic materials with the same formability and durability, since they detected that solid electrolyte should be used rather than the molten one was more convenient.

In 1955, Willard Thomas Grubb used a sulphonated polystyrene ion-exchange membrane as the electrolyte. In 1958, Leonard Niedrach deposited platinum on to this membrane, and final devise is known as "Grubb-Niedrach fuel cell". This device was supported and was sponsored by NASA to develop for Gemini space project.

In 1960, Grubb and Niedrach's and in 1964, Grubb and Michalske's worked on Bacon Cell and for the first time they improved the experiment by proving that the electrochemical oxidation of hydrocarbons was possible by using platinum electrodes below $150^{o}C$.

As a consequence of the oil crises in Cold War years, search for alternative energy sources gained importance and speed. In the early 1960s, Aircraft and Engine

Manufacture Company licensed Alkaline Fuel Cell experiment for the Apollo spacecraft fuel cells and they have started to use in U.S. space missions.

In between 1967-1975, phosphoric acid fuel cell discovery was achieved by Pratt and Whitney aircraft division. In this prototype, hydrogen produced by using the natural gas and liquid fuels. However, phosphoric acid has a poor electrical conductivity. PAFCs were slow developing technology then fuel cell devices.

Throughout the 1970s and 1980s fuel cell technology started to be more importance because of the increase of energy need. This necessity directed the scientists to find out more convenient energy source materials. At that point, improvement of fuel cell technology was accelerated.

In 1993 fuel cells get employed by automobile manufacturers. First marketable fuel cell-powered vehicle was developed by Ballard, the Canadian company using PEM technology.

1.4. TYPES OF FUEL CELLS

Fuel cells can be classified according to the different parameters such as the type of fuel and electrolyte that are used in the system. According to the kind of electrolyte, five main types of fuel cells exist. Their properties (type, electrolyte, operating temperature, efficiency, applications, advantages and disadvantages of fuel cells) were given in the table in Figure 1.3.

1. Polymer Electrolyte Membrane (PEM) Fuel Cells
2. Alkaline Fuel Cells
3. Phosphoric Acid Fuel Cells
4. Molten Carbonate Fuel Cells
5. Solid Oxide Fuel Cells

Table 1.1. Comparison of fuel cell technology

Fuel Cell Type	Common Electrolyte	Operating Temperature	Typical Stack Size	Efficiency	Applications	Advantages	Disadvantages
Polymer Electrolyte Membrane (PEM)	Perfluoro sulfonic acid	50-100°C 122-212° typically 80°C	< 1kW-100kW	60% transportation 35% stationary	• Backup power • Portable power • Distributed generation • Transporation • Specialty vehicles	• Solid electrolyte reduces corrosion & electrolyte management problems • Low temperature • Quick start-up	• Expensive catalysts • Sensitive to fuel impurities • Low temperature waste heat
Alkaline (AFC)	Aqueous solution of potassium hydroxide soaked in a matrix	90-100°C 194-212°F	10-100 kW	60%	• Military • Space	• Cathode reaction faster in alkaline electrolyte, leads to high performance • Low cost components	• Sensitive to CO_2 in fuel and air • Electrolyte management
Phosphoric Acid (PAFC)	Phosphoric acid soaked in a matrix	150-200°C 302-392°F	400 kW 100 kW module	40%	• Distributed generation	• Higher temperature enables CHP • Increased tolerance to fuel impurities	• Pt catalyst • Long start up time • Low current and power
Molten Carbonate (MCFC)	Solution of lithium, sodium, and/or potassium carbonates, soaked in a matrix	600-700°C 1112-1292°F	300 kW-3 MW 300 kW module	45-50%	• Electric utility • Distributed generation	• High efficiency • Fuel flexibility • Can use a variety of catalysts • Suitable for CHP	• High temperature corrosion and breakdown of cell components • Long start up time • Low power density
Solid Oxide (SOFC)	Yttria stabilized zirconia	700-1000°C 1202-1832°F	1 kW-2 MW	60%	• Auxiliary power • Electric utility • Distributed generation	• High efficiency • Fuel flexibility • Can use a variety of catalysts • Solid electrolyte • Suitable for CHP & CHHP • Hybrid/GT cycle	• High temperature corrosion and breakdown of cell components • High temperature operation requires long start up time and limits

1.5. THE DIRECT METHANOL FUEL CELLS

Direct methanol fuel cell (DMFC) is a subset of polymer electrolytes fuel cell (PEM). Methanol is used as a fuel resource in DMFC that can be reacted with oxygen (or air) to be directly converted into electrical energy. Two catalytic electrodes are separated by a proton exchange membrane (PEM) which conducts protons from anode to cathode, while diffusion of other compounds is prevented.

Reaction takes place in two part. At anode part of the cell aqueous solution of methanol is electrochemically oxidized into carbon dioxide and protons (hydronium ions) which diffuse through the membrane to cathode. At cathode part, protons are converted to water by the reduction of oxygen. Water is consumed in anode whereas producing in cathode of the fuel cell. During the process, metal catalyst is used to provide anodic and cathodic reactions. Schematic representation of DMFC is shown in Figure 1.4.

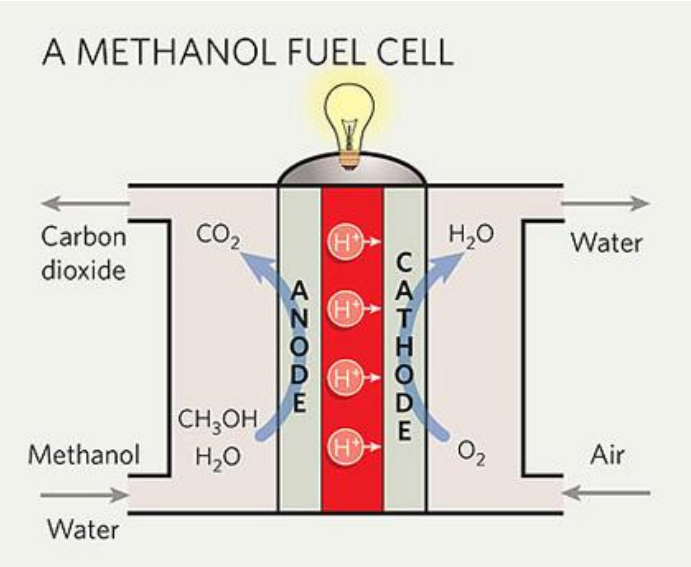

Figure 1.4. Schematic representation of a DMFC[82].

Both reactions at the anode and cathode are shown below. The overall reaction is the conversion of methanol and dioxygen to carbon dioxide and water.

Anode Reaction:

$$CH_3OH + H_2O \rightarrow 6\ H^+ + 6\ e^- + CO_2$$

Cathode Reaction:

$$3/2\ O_2 + 6\ H^+ + 6\ e^- \rightarrow 3\ H_2O$$

Overall Reaction:

$$CH_3OH + 3/2\ O_2 \rightarrow CO_2 + 2\ H_2O$$

In addition to overall reaction, production of byproducts also occurs during the process. Methanol electro-oxidation on the surface of catalyst is an essential part of the process. Scientists tried to analyze the methanol absorption on the surface of catalyst for many years and reached to the following resulted equations:

Dehydrogenation of methanol:

$$CH_3OH \rightarrow COH_{ads} + 3\ H^+ + 3\ e^-$$

Oxidation of these adsorbed species:

$$COH_{ads} + H_2O_{ads}\ (\text{ or } OH_{ads}) \rightarrow CO_2 + 3\ H^+ + 3\ e^-$$

Sometimes carbon monoxide also adsorbed onto platinum surface which could not be oxidized. Consequently, they prevent methanol molecules to adsorb and proceed to the reaction which reduce the reaction efficiency. Therefore adsorbed CO on the surface of catalyst is known as poison. The estimated mechanism for methanol oxidation reaction is given below:

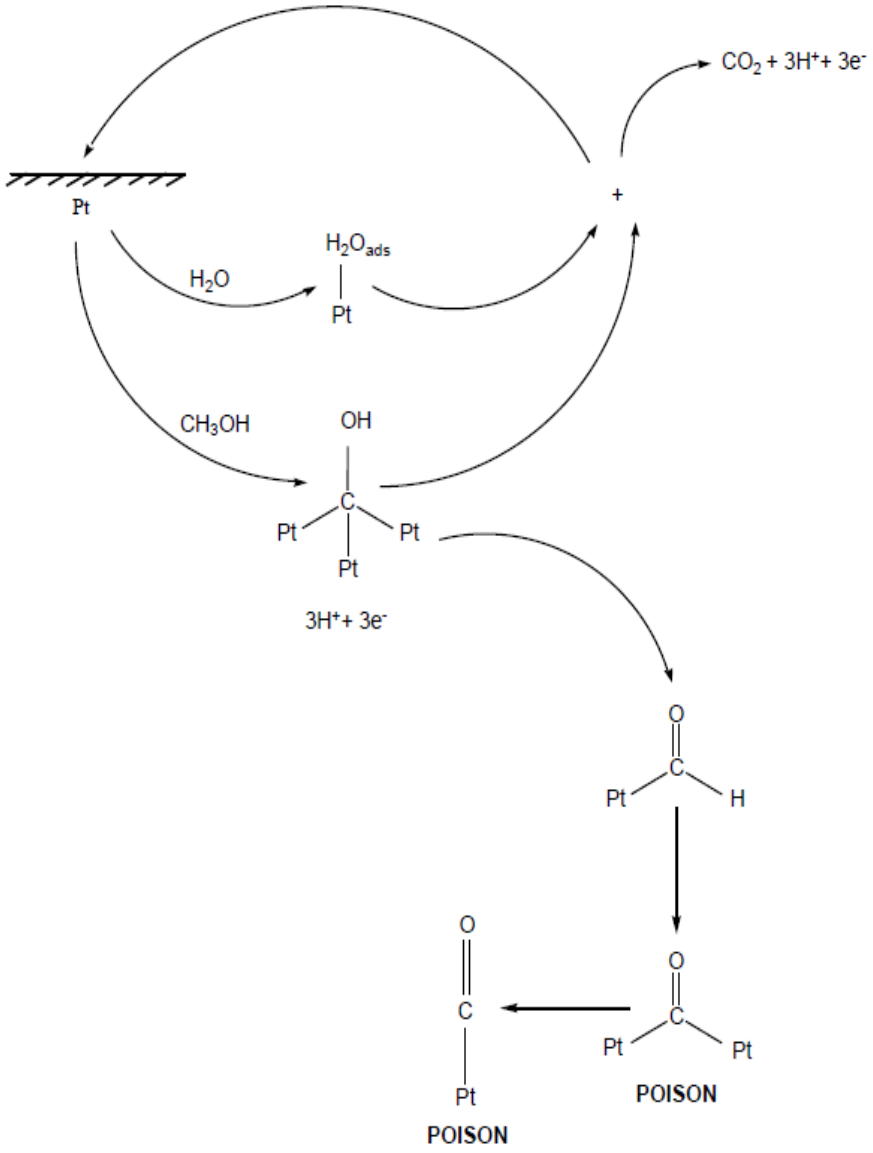

Figure 1.4. Methanol electrooxidation mechanism and poisoning on pure platinum surface in acid electrolyte[83].

Since the numerous advantages exist, it is assumed that DMFCs are one of the possible alternative power sources for future technology. Those can be ordered as below:

- Green source which is environmental friendly with the absence of by products such as sulfur and nitrogen species (except for CO_2).
- No fuel storage problems.
- Simplicity of the handling and transport makes them preferable.
- Direct electricity production from fuel with a high efficiency
- High energy density (~20 MJ/kg)..
- No need for reforming of methanol,
- Well suited for portable device applications with minimized size and weight,
- Low operating temperature.

Beside the advantages of the DMFC, there are also some limitations such as:

- Methanol is electrochemically inactive, therefore the catalyst is needed.
- DMFC is expensive electrochemical device because precious metals are used to prepare catalysts.
- Reaction rate of DMFCs are slow
- Toxicity of methanol draws the researchers to take necessary precautions.
- Acid electrolyte must be used to avoid the carbonate formation, resulting corrosion of metal which causes to reduce the reaction rate at the cathode.
- High metal content of the catalyst makes the device vulnerable for catalyst poisoning resulting from CO adsorption on surface on metal catalyst. Most widely accepted theories has been put forward by Breiter[67].

CHAPTER 2

EXPERIMENTAL

2.1. SYNTHESIS OF CATALYSTS

2.1.1. SYNTHESIS OF CATALYST Ia

0.0808 g (0.24 mmol) of $PtCl_4$ was weighed (%99 Alfa) and dissolved in 120 ml deionized water and stirred for 20 minutes. Then, 0.22 mmol (0.0112 M) of freshly prepared $NaBH_4$ (reducing agent) solution was added dropwise to accomplish the reduction of Pt complex. It is waited to color change from yellow to black and to end of hydrogen gas evolution (bubbling). After a few minutes, 0.24 mmol of heptanamine surfactant in 120 ml of toluene solution was added. After addition of toluene, separation into two phases was achieved and provided to gather of Pt nanoparticles into the intermediate phase. Then, 1.4 ml of 1 M NaOH solution was added into the black solution to achieve the better phase separation and stirred for two hours to complete reaction (During all these processes and reactions, high purity Argon atmosphere was performed). First, obtained solution was centrifuged during 30 minutes. Thereafter, washing process is performed 7 times with dry ethanol to remove excess amines from solution. Finally the product was dried under vacuum at room temperature.

2.1.2. SYNTHESIS OF CATALYST IIa

0.0808 g (0.24 mmol) of $PtCl_4$ (%99 Alfa) was dissolved in 120 ml deionized water by stirring for 20 minutes. Then 2.4 mmol (2 M) of N_2H_5OH solution was added to the solution by dropwise till the reduction of Pt complex. During this process, the change in the color from yellow to grayish black was observed. Afterwards, 120 mL of toluene including 0.24 mmol of heptanamine was introduced into the solution. Then, the same procedure was followed as in synthesis of Cat Ia.

2.1.3. SYNTHESIS OF CATALYST IIIa

0.24 mmol of $PtCl_4$ complex was dissolved in 120 ml of deionized water. The solution was heat up gradually to 70°C for providing better reduction, then the pH value of solution was adjusted to 9-10 by adding 2.5 M NaOH solution. To start the reduction process, 0.48 mmol of formaldehyde is added to this solution then, stirred under the high purity argon atmosphere until to observe the color change. Afterwards, 0.24 mmol of heptanamine surfactant in 120 ml of toluene solution was added. Then the procedure was maintained by the same steps as mentioned in 2.1.1.

2.1.4. SYNTHESIS OF CATALYSTS Ib, IIb, IIIb, Ic, IIc, IIIc

The same methods were followed to prepare Cat b and c by using appropriate amount of N-methylheptanamine with the reducing agents of sodium borohydride, hydrazinum hydroxide and formaldehyde respectively and the name of catalysts, surfactant and the reducing agents are given in Table 3.

Table 2.1. Reducing agents and surfactants that was used to synthesis platinum nanoparticle catalysts

Catalysts	Reducing agents	Surfactants
Cat Ia	Sodium borohydride	1-heptanamine
Cat Ib		N-methyl-1-heptanamine
Cat Ic		N,N-dimethyl-1-heptanamine
Cat IIa	Hydrazinum hydroxide	1-heptanamine
Cat IIb		N-methyl-1-heptanamine
Cat IIc		N,N-dimethyl-1-heptanamine
Cat IIIa	Formaldehyde	1-heptanamine
Cat IIIb		N-methyl-1-heptanamine
Cat IIIc		N,N-dimethyl-1-heptanamine

2.2. ELECTRODE PREPARATION

0.5 mL of Nafion (Aldrich, 5 wt %), 0.15 mL of N, N-dimethyl formamide (Merck, 99.5 %) and 2.5 mL of distilled water was added to 36.78 mg carbon supported powder catalyst and centrifuged for 72 hours to obtain homogenous solution (The platinum containing sample to carbon support ratio is 1:10). Resulting solution was stirred in ultrasonic bath for a few days to disperse solution well. 50 μL of this solution was dropped on a glassy carbon with diameter of 0.7 cm. Then drying process was applied at 40°C for 20 minutes, at 65°C for 20 minutes and finally at 100°C for 1 hour to provide good 'adhesion' of the catalyst to the surface of the glassy carbon electrode[61]. This is used as a reference electrode.

2.3. DETERMINATION OF PLATINUM CONTENT IN THE CATALYSTS

Leeman Lab inductively coupled plasma spectroscopy (ICP-OES) from METU Central Lab was employed to determine the percentage of platinum contenct in sythesized catalysts.

2.4. CHARACTERIZATION TECHNIQUES

2.4.1. CYCLIC VOLTAMMETRY (CV)

Cyclic voltammetry is the analytical technique that provides qualitative information about electrochemical properties of an analyte in solution. Charge transfer between an electrode and a species in solution is provided by electrolysis, which is explained as below:

- Reactant moves to the interface, capable of receiving an electron from the electrode diffuses to the surface.

- Electron transfer can then occur via quantum mechanical tunnelling between the electrode and reactant.

- The products moves away from the electrode to allow fresh reactant to the surface. Electron transfer occurs from the electrode to the redox species and current is produced at the surface which caused by the migratin of ions.

Cyclic voltammetry is a three electrode system :

1. Reference Electrode (RE):

Required to measuring the potential of the working electrode (WE). This measurement can be done by fixing the potential of stable reference electrode (RE).

2. Counter Electrode (CE):

Allows the reaction at the WE to take place with a respective reverse reaction; for example, for every electron intercepted by oxidation at the WE, one electron reduction process has to take place at the CE (typically the reduction of protons to hydrogen).

3. Working Electrode (WE):

Electrochemical reaction of interest can be examined in working electrode. The potential of the working electrode is controlled by a reference electrode such as a saturated calomel electrode (SCE).

A typical cyclic voltammogram is illustrated in Figure 2.1.

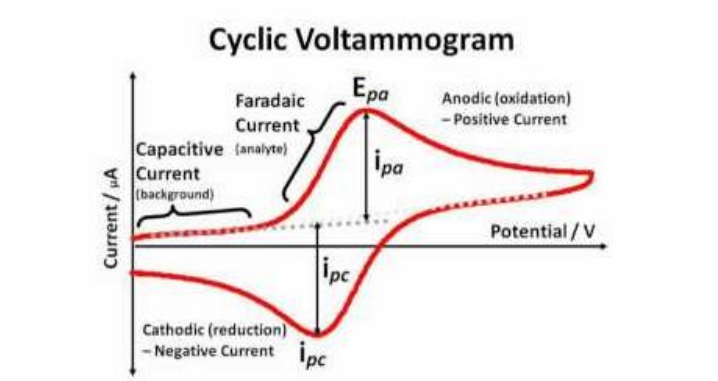

Figure 2.1. Typical cyclic voltammogram.

This electroanalytical technique has been widely used for redox reactions, determining the stability of reaction products, intermediates species in reactions, kinetics of electron transfer and the reaction reversibility. Mostly, reproducible results can be obtained in the range of suitable potentials. In this study, microcomputer–controlled potentiostat/galvanostat, Solartron 1285 device was used to measure cyclic voltammograms of catalysts.

2.4.2. X-RAY DIFFRACTION (XRD)

X-ray diffraction is a modern spectrographic technique which relies on the dual wave/particle nature of X-rays and provide information from qualitative and quantitative analysis of the structure of crystalline materials. XRD can be used to differentiate between materials by identifying and characterizing the compounds based on their diffraction pattern, since the most crystalline materials have unique x-ray diffraction patterns.

By using XRD, types and nature of crystalline materials, degree of crystallinity, amount of amorphous content, microstrain & size and orientation of crystallites can be analysed.

In the base of working principle, the sample is irradiated with a beam of monochromatic X-rays, which interacts with a target material. X-rays from atoms within the target material scatters and undergoes to constructive and destructive interference process which is called diffraction. This diffraction can be described by Bragg's Law, $n\lambda=2d \sin \theta$. Simple schematic representation of XRD device system is represented in Figure 2.2.

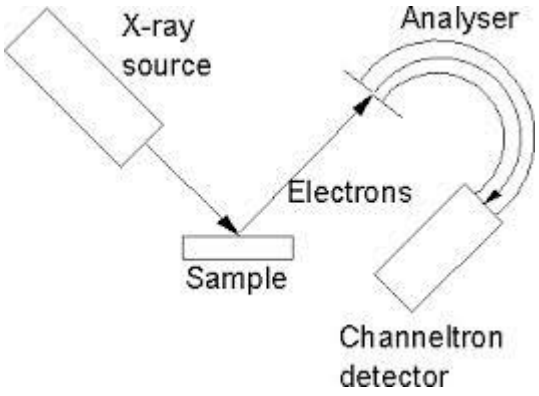

Figure 2.2. Simple schematic representation of XRD device system.

This technique has numerious advantages as:

- Non-destructive analysis,
- No sample preparation is required,
- Qualitative and quantitative analyses can be done,
- High efficiency (throughput) property, and
- Possibility to distinguish chemical compounds, polymorphic forms, and mixed crystals.

In this study, by using Rigaku diffractometer, with an Miniflex +θ-θ high resolution goniometer X-ray diffraction was carried out. Cu Kα radiation with λ= 1.54056 A□ operated at 20 kV and 30 mA.

2.4.3. TRANSMISSION ELECTRON MICROSCOPY (TEM)

In case of excitation of electrons to high energy levels, they can scatter or backscatter elastically or inelastically by interacting strongly with atoms. They may also cause many interactions, source of different signals such as X-rays, Auger electrons or light. Some of those signal can be used in transmission electron microscopy (TEM),

A Transmission Electron Microscope (TEM) utilizes energetic electrons to provide morphologic, compositional and crystallographic information on samples. TEM is a powerful technique for characterization of structures of materials that uses high energy electrons to penetrate through a sample, especially in identifying and quantifying the chemical and electronic structure of individual nanocrystals. This offers the possibility of carrying out diffraction from nano-sized materials. Schematic diagram for a transmission electron microscope can be seen from Figure 2.3.

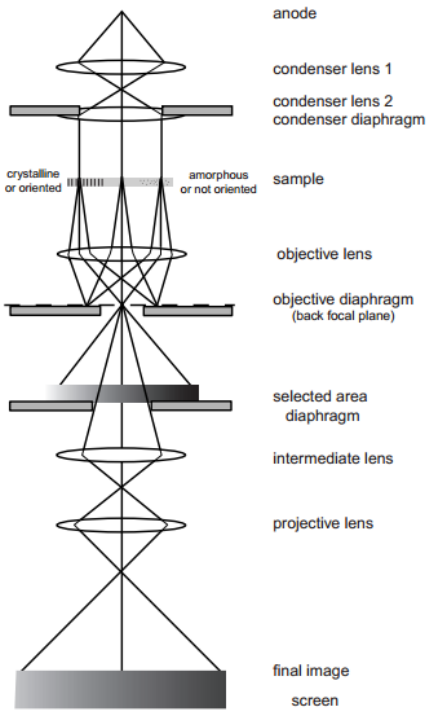

Figure 2.3. Schematic diagram for a transmission electron microscope (TEM).

This technique provides us for the analyses of structural properties (as size distribution of entities, area density, structural defects), chemical properties (like composition, modification and interface sharpness), electronic properties and magnetic properties of materials.

Five main components exist in a transmission electron microscope:

1. Electron optical column,
2. Vacuum system,
3. Lens supplies,
4. High voltage generator, and
5. Control software.

In this study, transmission electron microoocopy (TEM) images were obtained by using JEOL-2100F at 200kV instrument. To prepare sample for TEM, 0.5 mg of Pt catalyst was dispersed into CCl_4 solution by ultrasonicating for ~ 30 minutes and a few drop of this solution were placed on 400-mesh copper grid, and was allowed for evaporation before analysis.

2.4.4. X-RAY PHOTOELECTRON SPECTROSCOPY (XPS)

X-ray photoelectron spectroscopy (XPS), which is known as ESCA (electron spectroscopy for chemical analysis) is a semi-quantitative technique that can provide us to determine the composition of material on the basis of photoelectric effect. This also provides to be informed about elemental and chemical state independent from the type of material.

Photoelectron spectroscopy functioned based on a single photon in/electron out process. The sample is exposed to X-rays and photoelectrons are emitted from the surface of material. The kinetic energy of these emitted electrons is identical for each element and determining the atomic composition of the sample can be analyzed, since the binding energies of the electron orbitals in atoms are also identical. Chemical state and quantitative information can be obtained by measuring the relative areas of those characteristic peaks. Figure 2. 4. illustrates schematic diagram for X-ray photoelectron spectroscopy.

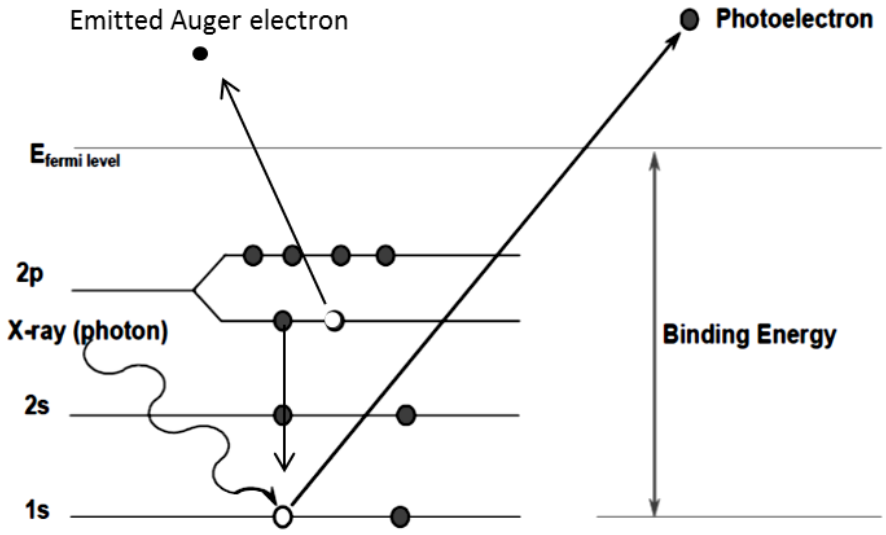

Figure 2.4. Schematic diagram for X-ray photoelectron spectroscopy (XPS).

In this study, a SPECS spectrometer was employed for XPS measurements. Mg Kα lines (1253.6 eV, 10 mA) was used as a source and C 1s line at 284.6 eV was used as reference. Gaussion Lorentz method is used for peak fitting analyses.

2.4.5. INDUCTIVELY COUPLED PLASMA SPECTROSCOPY (ICP)

An inductively coupled plasma is a promising technique which is used to detect and analyse trace and ultra-trace elements. It is the common high-temperature ion source with multi-elemental analytical method. Characterization of different materials both organic and inorganic is possible. After 1983 this technique has gained general importance in many laboratories[68]. In these days ICP-OES is used in variety of fields such as science and industry.

Elemental content of a material (except noble gases and halogens such as C, H, O and N) can be measured by ICP-OES. There are six components exist such Sample introduction, energy source, spectrometer, detector, electronics, software. Schematic representation of working principle of ICP-OES is illustrated in Figure 2.5.

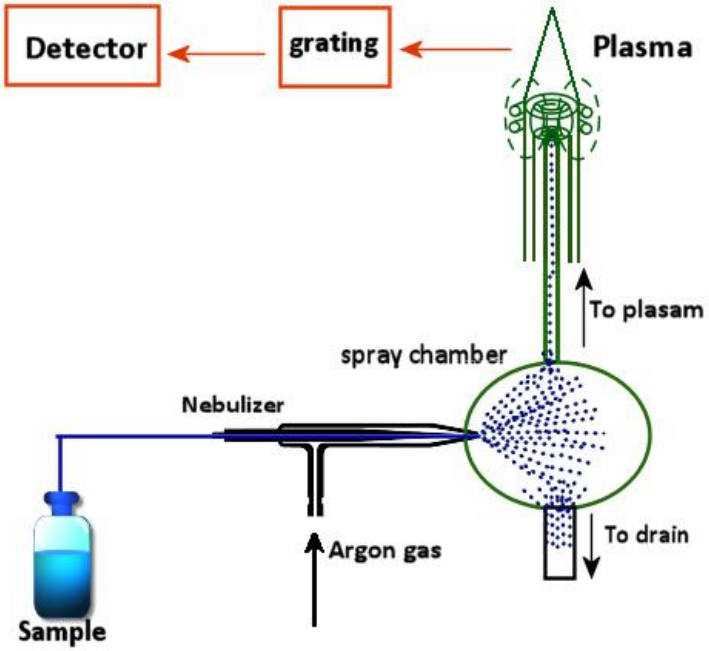

Figure 2.5. Principle of sample introduction in ICP-OES.

Wide usage area of this technique is due to the advantages which are detailed below:

- Opportunity to determine up to 70 elements,
- Higher atomization temperature around 6000-10000 K
- The high ion density,
- More inert environment,
- Low background emission and less susceptible to matrix interferences,
- Applicable for refractory elements,
- High stability, good accuracy and precision,
- Detection limits are excellent for most elements,

In this study, to determine the amount of platinum in the catalysts, Leeman Lab ICP-OES was utilized.

2.4.6. BRANAUER-EMMETT-TELLER (BET) SURFACE AREA ANALYSIS

BET analysis provides precise specific surface area determination of materials by physical adsorption of gas molecules on a solid surface. Specific surface area evaluations measures the external surface area and pore area of materials, as well as pore volume and area distributions.

As is well known, the BET theory[69] is based on an over-simplified model of physisorption[70]. The concept of the theory based on:

1) Adsorbtion of gas molecules on solid surface,

2) No interaction occurs between each adsorption layer, and

3) the Langmuir theory can be applied.

The resulting BET equation is given below:

$$\frac{1}{W\left(\left(P_0/P\right)-1\right)} = \frac{1}{W_m C} + \frac{C-1}{W_m C}\left(\frac{P}{P_0}\right)$$

P/P_0 : Relative pressure

W_m: Weight of adsorbate as monolayer

W: weight of gas adsorbed

C: BET constant

This technique is useful for variety of other applications such as medical, environmental, pharmaceutical, cosmetic, textile and ceramic industry. In addition, it is widely used in nanotechnology and fuel cell technology.

CHAPTER 3

RESULTS AND DISCUSSION

3.1. INDUCTIVELY COUPLED PLASMA SPECTROSCOPY AND BET SURFACE AREA ANALYSIS

Inductively coupled plasma spectroscopy (ICP) was utilized to define the amount of platinum content in the sample by using the Leemna Lab ICP-OES spectroscopy. The measurements were done on the samples which do not contain carbon support. It was found that most of the samples composed of platinum, ~90 %, and small amount of residue, ~ 10 %, which can be seen from Table 3.1. The residue was most probably unremoved surfactants and/or reducing agent which could not be discharged during washing process. These ICP results was used to record cyclic voltammogram in mA/mg platinum instead of mA/cm^2.

Brunauer, Emmnett and Teller (BET) technique was use to determine the surface area of sample which do not include carbon support. As can be seen from Table 3.1., Cat II has the smallest surface area ~ 6 m^2/g sample, while Cat III has the largest one, ~ 38.73 m^2/g sample. Cat II possesses an intermediate value, ~ 29.24 m^2/g sample. Except Cat II, the largest surface area results were obtained for Cat Ic and Cat IIIc for Cat I and Cat III, respectively. In order to interpret these results properly, XRD and TEM outcomes should be considered, given in the next section.

Table 3.1. ICP & BET results of all catalysts

Catalysts	Platinum %	Surface Area (m^2/g)	Average Surface Area (m^2/g)
Cat Ia	93.4 ± 1.0	27.58	
Cat Ib	88.3 ± 1.1	27.88	29.24
Cat Ic	92.5 ± 0.4	32.25	
Cat IIa	88.5 ± 0.6	5.44	
Cat IIb	87.3 ± 1.0	6.28	6.00
Cat IIc	89.2 ± 0.6	6.22	
Cat IIIa	92.3 ± 0.5	36.80	
Cat IIIb	92.0 ± 0.7	36.50	38.73
Cat IIIc	93.8 ± 0.5	42.88	

3.2. X-RAY DIFFRACTION (XRD) AND TRANSMISSION ELECTRON MICROSCOPY (TEM)

X-ray diffraction (XRD) was employed to determine the crystal structure and the crystallite size of platinum for all catalysts and XRD patterns of all catalysts are given in Figure 3.1. As can be seen from the figure, the characteristic features of face-centered cubic (fcc) structure of platinum were observed at about 39.9, 46.35, 67.75 and 81.25 (2θ) which correponds to (111), (200), (220) and (311) platinum planes, respectively. In addition to crystal structure, on average crystallite size of platinum were also defined from XRD data. For this purpose, the Scherrer formula was used. The formula is:

$$d(Å) = k.\lambda / \beta. \cos\theta$$

where d = average particle size,

k = Scherrer constant (0.9),

λ = wavelength of the incident X-ray (1.54056 Å),

β = full width half – maximum of XRD peak in rad, and

θ = the angle that correspond to the peak position at maximum height.

The average crystallite size of platium nanoparticles were found to be ~5.3, ~5.5, ~5.2, ~4.1, ~4.9, ~4.5, ~5.2, ~4.1 and ~4.9 nm for catalyst Ia, Ib, Ic, IIa, IIb, IIc, IIIa, IIIb and IIIc, respectively, Table 3.2. These results indicate that there is not much platinum nanoparticle size difference between the catalysts. However, it should be kept in mind that if there is a large size difference between the particles, XRD may not be appropriate technique. Therefore, these results should be confirmed by other techniques, such as TEM.

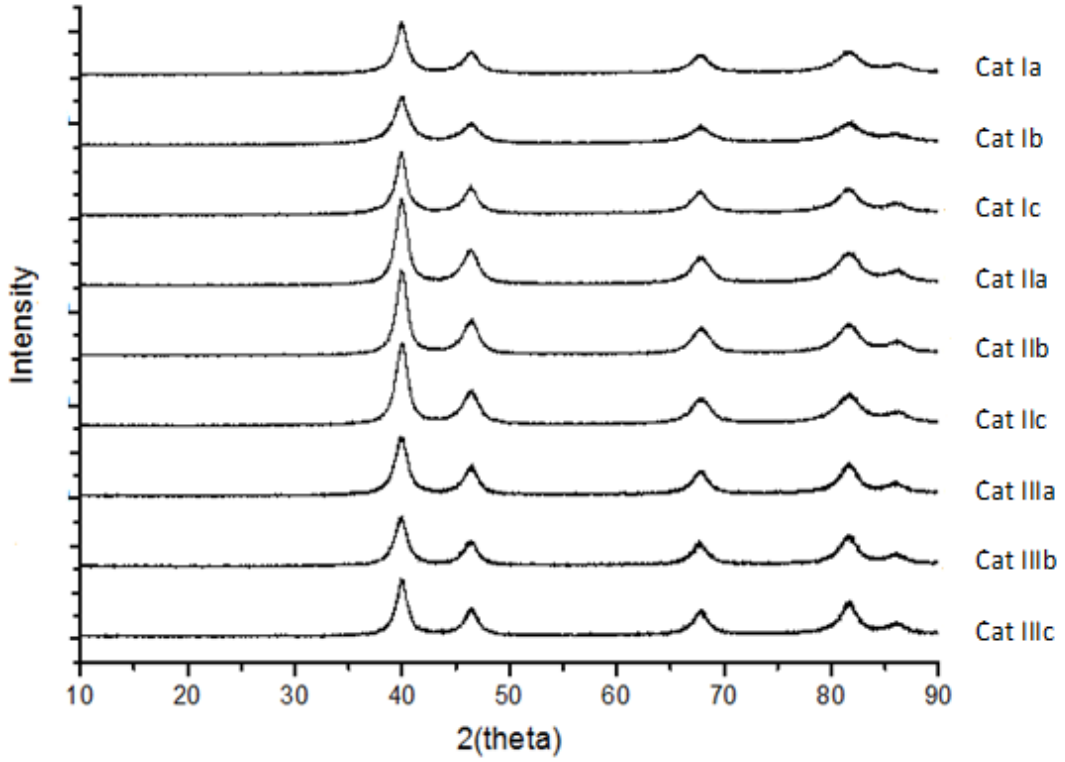

Figure 3.1. XRD pattern for all of the catalsyts

Table 3.2. Average particle size of small platinum nanoparticles estimated from a) XRD and b) TEM. Agglomerated particles were not considered.

Catalysts	a	b
Cat Ia	~ 5.3 nm	~ 4.9 ± 1.0 nm
Cat Ib	~ 5.5 nm	~ 5.1 ± 0.8 nm
Cat Ic	~ 5.2 nm	~ 4.9 ± 0.9 nm
Cat IIa	~ 4.1 nm	~ 4.0 ± 0.7 nm
Cat IIb	~ 4.9 nm	~ 4.6 ± 0.6 nm
Cat IIc	~ 4.5 nm	~ 4.6 ± 0.8 nm
Cat IIIa	~ 5.2 nm	~ 4.8 ± 0.7 nm
Cat IIIb	~ 4.1 nm	~ 4.3 ± 0.8 nm
Cat IIIc	~ 4.9 nm	~ 4.9 ± 0.7 nm

Transmission electron microscopy was used to determine the average and individual size of platinum nanoparticles and their distribution on carbon support. In general, it was observed that platinum nanoparticles were uniformly distributed on carbon support and average particle size of platinum particles were calculated by considering about 500 particles from different region for all catalysts and size distribution histograms was plotted in Figure 3.2. It was found that the average size of platinum nanoparticles was ~4.9, ~5.1, ~4.9, ~4.0, ~4.6, ~4.6, ~4.8, ~4.3 and ~4.9 nm for the catalysts Ia, Ib, Ic, IIa, IIb, IIc, IIIa, IIIb and IIIc, respectively, Table 3.2. and these results were consistent with XRD results.

Beside size, TEM technique provides an opportunity to monitor the shape of the individual particles. The TEM images revealed that Cat II and III have spherical platinum nanoparticles, Figure 3.3., while Cat I has cubic form of platinum nanoparticles, Figure 3.4. The same conclusions were observed by Yang [42,43] and at. all., they also used sodium borohydride as a reducing agent. Besides the individual particles, it is also possible to compare the number of small particles between the groups in a rough manner, for instance Cat III has the largest number of small particles while Cat II has the smallest ones. Using this information, it is possible to estimate relative surface area of catalysts, for instance, it should be increases from Cat II, I to III. To approve this observation, BET analyses have been achieved, as given in the previous section, Cat III has the highest average surface area (38.73 m^2/g sample), while Cat II has the smallest (6.00 m^2/g sample), Table 3.1., which is in good agreement with the TEM results' estimation.

In addition to these small platinum particles, agglomerated large particles were also observed for all catalysts. Obviously, agglomerated particles were composed of small nanoparticles.The number and morphology of these large particles changes from one group to another, as given for small nanoparticle case, for instance the shape of large particles in Cat I a-c were not in perfect spherical form as shown in Figure.3.5, but it is still possible to calculate the rough size of these large particles such as it is between 20-150 nm. On the other hand, most of the particles were large, spherical and compact in Cat II with a size of 20-300 nm, Figure 3.6. Similar spherical and

agglomerated particles (20-200 nm) were observed for Cat III, Figure. 3.7., but not as dense as Cat II.

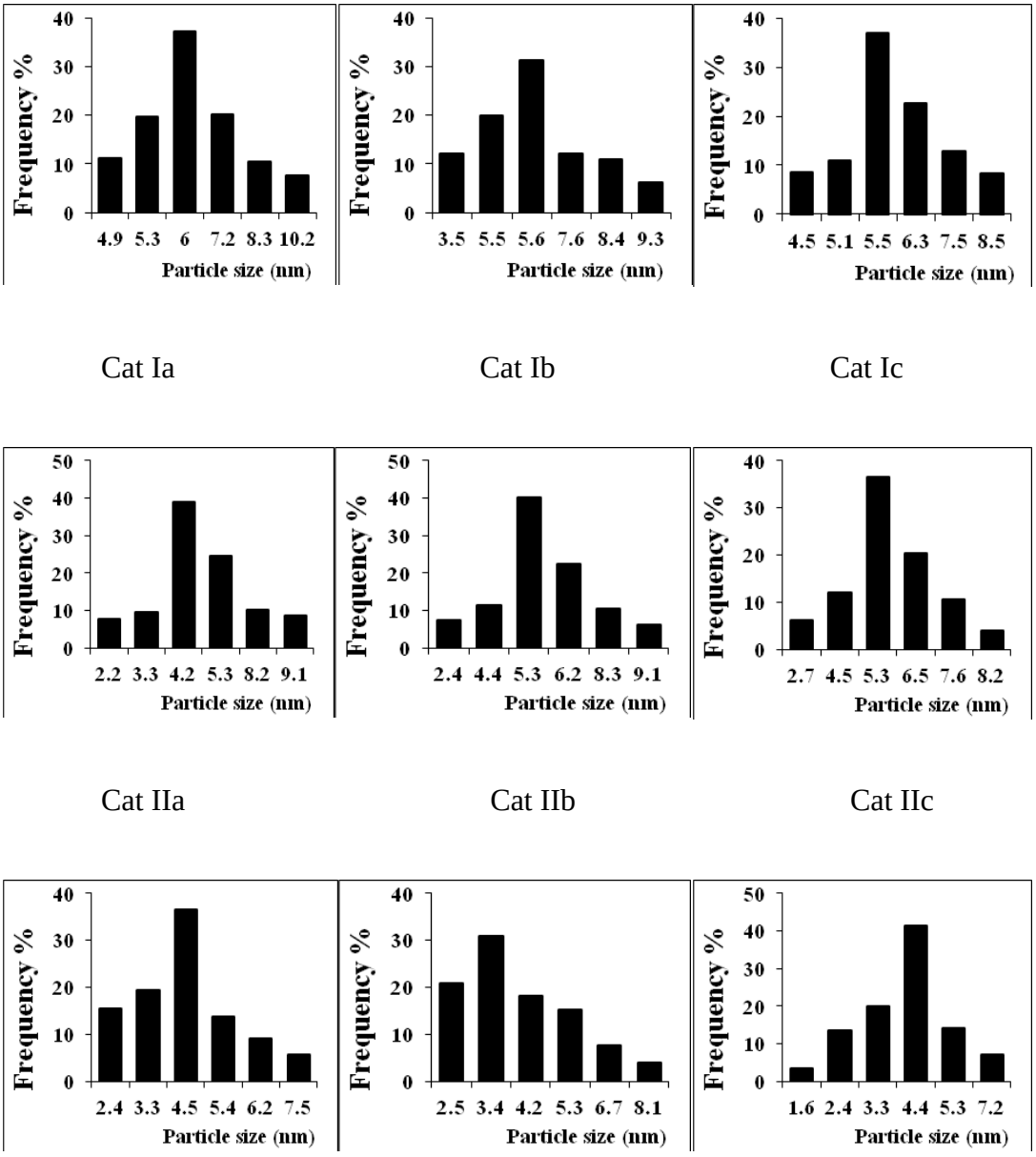

Cat Ia Cat Ib Cat Ic

Cat IIa Cat IIb Cat IIc

Cat IIIa Cat IIIb Cat IIIc

Figure 3.2. The size distribution histograms of platinum nanoparticles in all catalysts, agglomerated particles were not included.

In summary ;

a) Cat I contains mostly small (~5 nm) cubic and formless agglomerated (~20–150 nm) platinum nanoparticles.

b) Cat II involves predominantly spherical, dense and large (~20-300 nm) platinum nanoparticles, in addition to few numbers of small nanoparticles (~5 nm).

c) Cat III includes usually small platinum nanoparticles, (~5 nm), besides large (~20–200 nm) and less dense platinum particles, compared to Cat II.

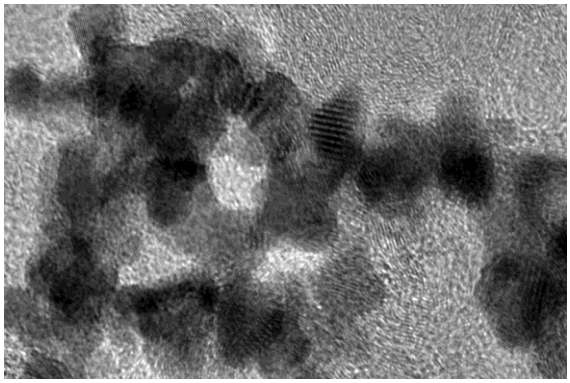

Figure 3.3. TEM image of the Cat IIb

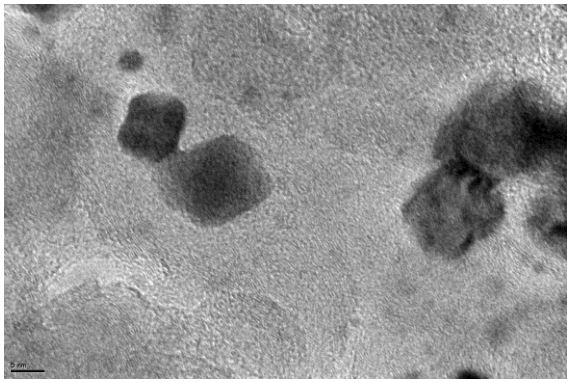

Figure 3.4. TEM images of the Cat Ia

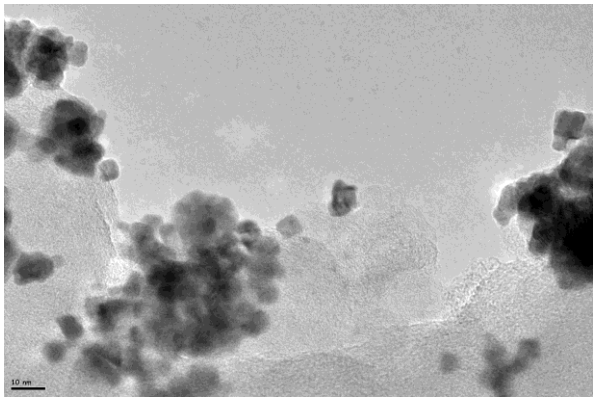

Figure 3.5. TEM image of the Cat Ia

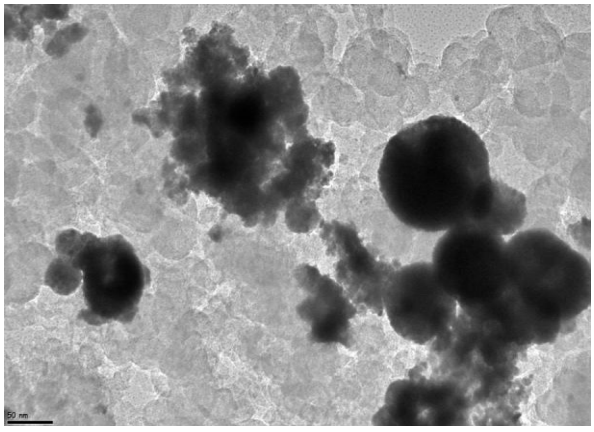

Figure 3.6. TEM image of the Cat IIb

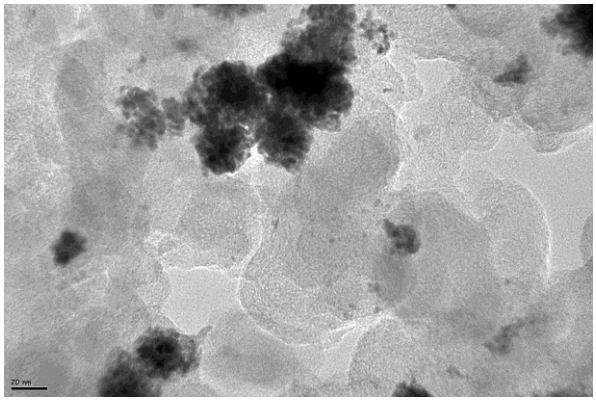

Figure 3.7. TEM image of the Cat IIIb

3.3. X-RAY PHOTOELECTRON SPECTROSCOPY (XPS)

XPS was employed to investigate the oxidation states of the elements and their relative amount in a given sample (In this study, sample is the catalyst which does not contain any carbon support). For this purpose, Pt 4f, O 1s and C 1s regions of the XPS spectra for all catalysts were recorded and Gaussian-Lorentzian method was used to analyze these peaks. C 1s peak at 284.6 eV was used as a reference point.

Pt 4f peak was evaluated by keeping 3.35 eV difference and 3:4 intensity ratio between $4f_{5/2}$ and $4f_{7/2}$ doublets as much as possible, Figure 3.8.a-i and the results were given in Table 3.3. The peak fitting analyses indicated that Pt 4f peak of all catalysts consist of two doublets, one at 71.1 eV ($4f_{7/2}$) and 74.2 eV ($4f_{5/2}$) and the other ones at 74.4 eV ($4f_{7/2}$) and 77.8 eV ($4f_{5/2}$) [24,29,55]. The first doublet belong to Pt(0) and the second one associated with Pt(IV) species, such as PtO_2 and/or $PtO(OH)_2$ and/or $Pt(OH)_4$, respectively.

Binding energy comparison within each group demonstrated that Cat a (Ia, IIa, IIIa) have lower value compare to others. This might be due to lower electron donation from platinum to the environment elements for Cat a, while electron moving from platinum to the other surrounding elements is greater for Cat b and c.

The Pt (0) / Pt (IV) relative ratio was calculated by using peak area under each doublet and it was found that the ratio changes between 64.5 / 35.5 and 69.6 / 30.4. Once again, when comparison is done within each group, it was noted that Cat b (Ib, IIb and IIIb) has the smallest Pt (0) to Pt (IV) ratio, while Cat c (Ic, IIc and IIIc) has the largest ratio. These results revealed that somehow the kind of surfactant affect the peak position and oxidation state ratio of platinum.

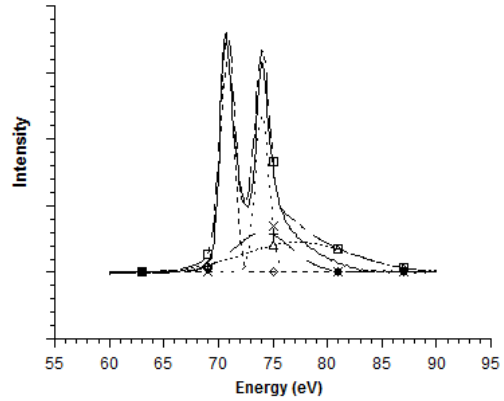

Figure 3.8.a. Pt $4f_{7/2}$ core binding energies, eV, for the Cat Ia

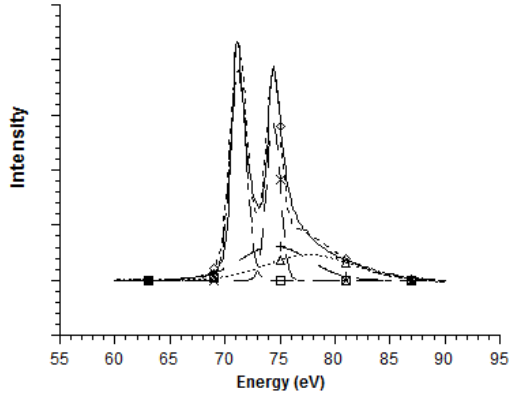

Figure 3.8.b Pt $4f_{7/2}$ core binding energies, eV, for the Cat Ib

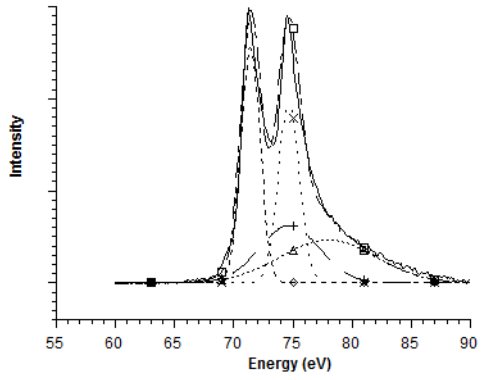

Figure 3.8.c. Pt $4f_{7/2}$ core binding energies, eV, for the Cat Ic

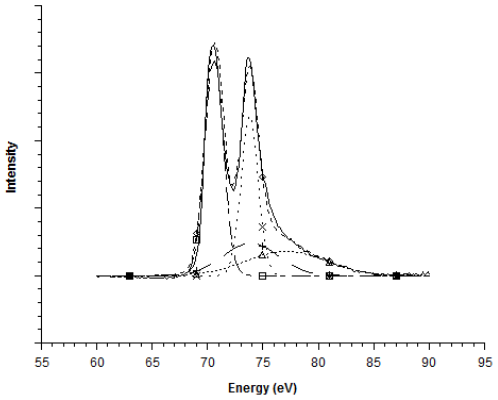

Figure 3.8.d. Pt $4f_{7/2}$ core binding energies, eV, for the Cat IIa

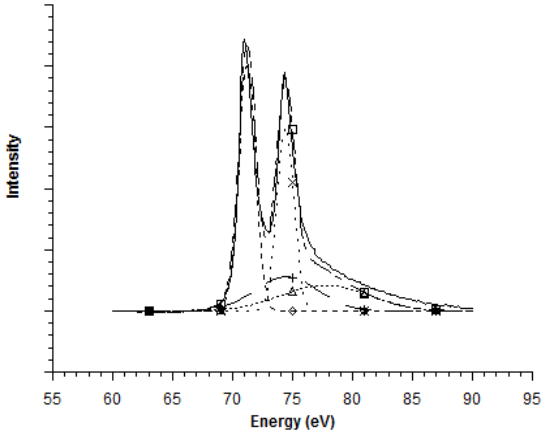

Figure 3.8.e. Pt $4f_{7/2}$ core binding energies, eV, for the Cat IIb

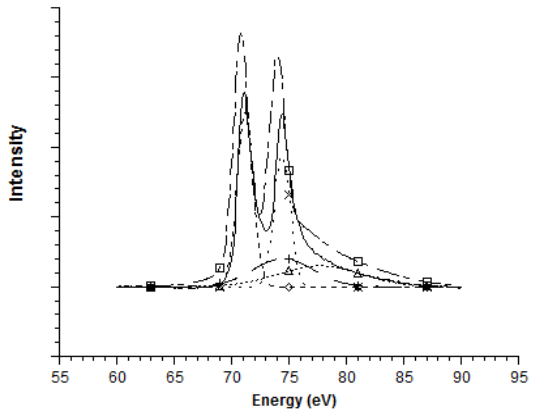

Figure 3.8.f. Pt $4f_{7/2}$ core binding energies, eV, for the Cat IIc

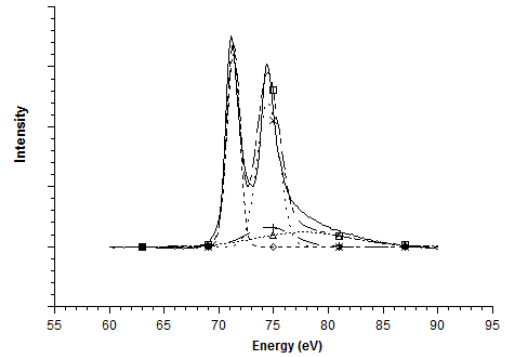

Figure 3.8.g. Pt $4f_{7/2}$ core binding energies, eV, for the Cat IIIa

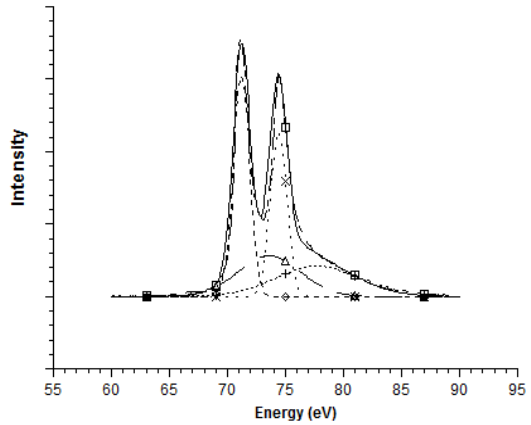

Figure 3.8.h. Pt $4f_{7/2}$ core binding energies, eV, for the Cat IIIb

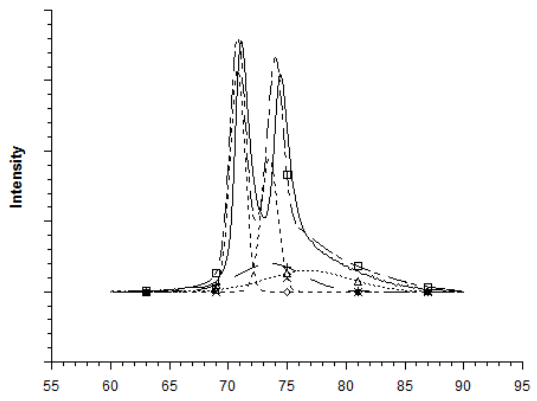

Figure 3.8.i. Pt $4f_{7/2}$ core binding energies, eV, for the Cat IIIc

Table 3.3. Pt $4f_{7/2}$ core binding energies, eV, in the prepared catalysts which do not contain carbon support and the relative intensities of species

Catalysts	Pt $4f_{7/2}$ (Pt(0))	Pt $4f_{7/2}$ (Pt(IV))	Pt(0) / Pt(IV)
Cat Ia	70.8 (67.7)	74.0 (32.3)	2.09
Cat Ib	71.2 (64.5)	74.4 (35.5)	1.82
Cat Ic	71.4 (69.6)	74.6 (30.4)	2.29
Cat IIa	70.6 (67.4)	73.8 (32.6)	2.07
Cat IIb	71.2 (66.4)	74.4 (33.6)	1.98
Cat IIc	71.2 (69.0)	74.4 (31.0)	2.22
Cat IIIa	70.8 (67.2)	74.1 (32.8)	2.05
Cat IIIb	71.2 (65.3)	74.4 (34.7)	1.88
Cat IIIc	71.3 (69.4)	74.5 (30.6)	2.27

Apart from Pt 4f region, O 1s region was also analyzed by Gaussian- Lorentzian peak fitting program. The analyses of the peak were achieved by keeping the half width of the peak at ~1.6 eV. Analyses indicated that O 1s peak consist of two peaks for all catalyst, one was obtained between 531.0 – 531.9 eV and the other one was observed between 532.0 – 532.8 eV, Figure 3.9.a-i., and the results were provided in Table 3.4. Previous studies indicated that the first peak could be due to adsorbed CO (CO_{ads})[72, 73] and most probably adsorbed OH (HO_{ads})[74] while the second peak could be owing to adsorbed H_2O (H_2O_{ads})[75, 76] on the surface of catalysts. The relative amount of HO_{ads} and H_2O_{ads} were also calculated by using peak area under each singlet and found out that the amount of H_2O_{ads} is ~15, ~10 and ~20 percent for Cat I, II and III, respectively. These results suggested that HO_{ads} / H_2O_{ads} ratio is most probably influenced by reducing agent but not surfactant, because there is no obvious relationship between the kind of surfactant and HO_{ads} / H_2O_{ads} ratio.

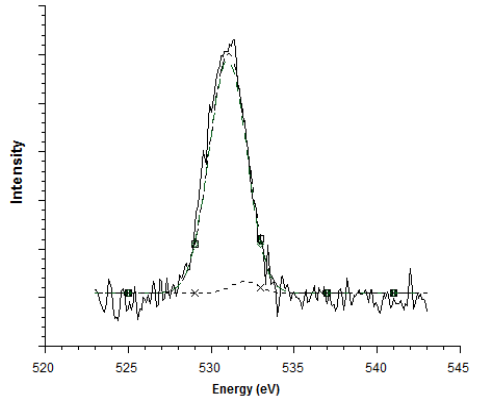

Figure 3.9.a. O 1s core binding energies, eV, for the Cat Ia

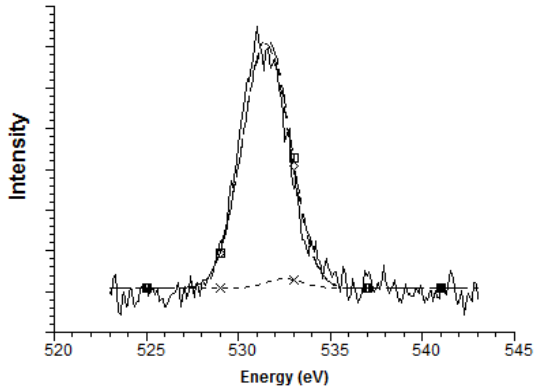

Figure 3.9.b. O 1s core binding energies, eV, for the Cat Ib

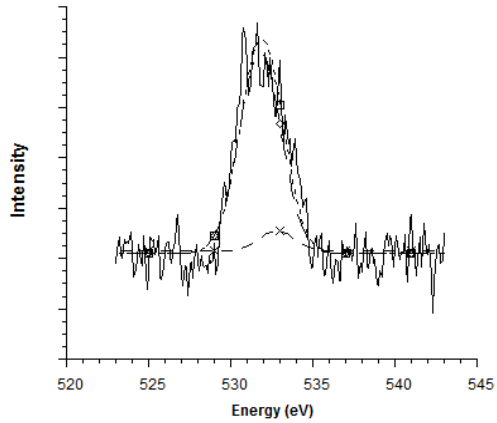

Figure 3.9.c. O 1s core binding energies, eV, for the Cat Ic

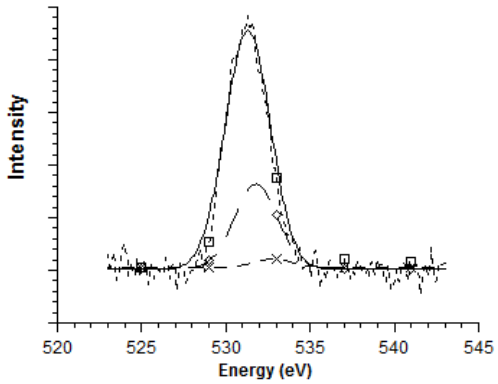

Figure 3.9.d. O 1s core binding energies, eV, for the Cat IIa

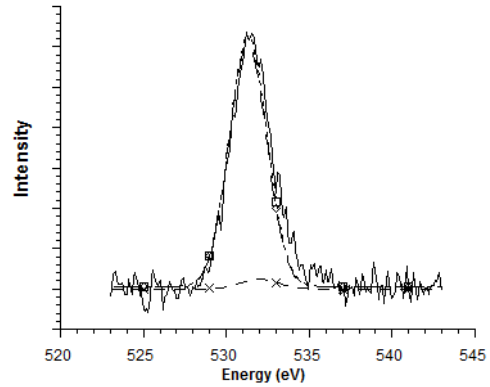

Figure 3.9.e. O 1s core binding energies, eV, for the Cat IIb

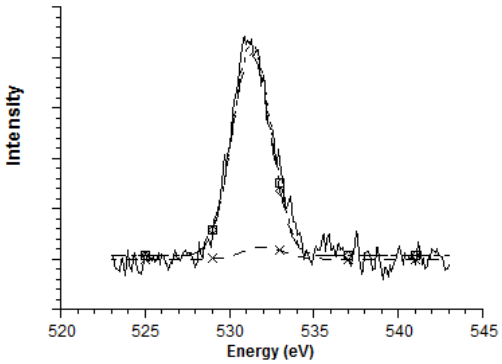

Figure 3.9.f. O 1s core binding energies, eV, for the Cat IIc

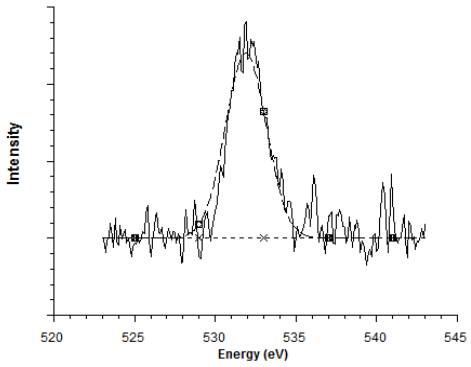

Figure 3.9.g. O 1s core binding energies, eV, for the Cat IIIa

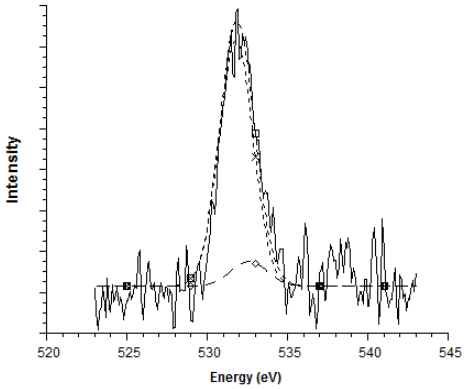

Figure 3.9.h. O 1s core binding energies, eV, for the Cat IIIb

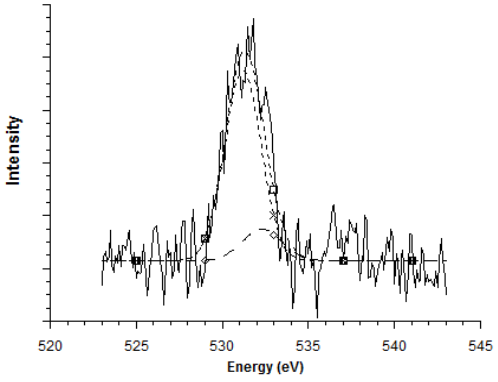

Figure 3.9.i. O 1s core binding energies, eV, for the Cat IIIc

Table 3.4. O 1s core binding energies, eV, in the prepared catalysts which contain carbon support and the relative intensities of species

Catalysts	O 1s (HO_{ads})	O 1s (H_2O_{ads})
Cat Ia	531.0 (83.4)	532.0 (16.6)
Cat Ib	531.5 (85.5)	532.5 (14.5)
Cat Ic	531.8 (83.9)	532.8 (16.1)
Cat IIa	531.3 (88.6)	532.0 (11.4)
Cat IIb	531.3 (90.0)	532.0 (10.0)
Cat IIc	531.3 (89.2)	532.0 (10.8)
Cat IIIa	531.9 (80.1)	532.8 (19.9)
Cat IIIb	531.8 (77.4)	532.6 (22.6)
Cat IIIc	531.2 (78.9)	532.3 (21.1)

In addition to Pt 4f and O 1s regions, C 1s region of XPS for all catalysts were also evaluated and the results were reported in Table. 3.5. As stresses begining of this section, the XPS measurements were done before addition of carbon support to the platinum containing sample. Therefore, C 1s peak does not coming from support material, but it is most probably due to hydrocarbon and/or partially crystalline carbon which could not be removed during washing process. This comment was supported by elemental analyses results. As given in ICP section, the prepared sample which does not contain carbon support, consist of ~ 90 % Pt and ~ 10 % residue which is most probably, partially crystalline carbon and/or hydrocarbons.

In general, C 1s peak consist of three peaks at ~ 284.2, ~ 258.3 and ~ 287.5 eV corresponding to sp^2 carbon atoms (C=C) in partially crystalline carbon[77], C in C-OH[78] or C-O[79, 80] and C in carbonyl (C=O)[39,79], respectively.

Table 3.5. C 1s core binding energies, eV, in the prepared catalysts which do not contain carbon and the relative intensities of species

Catalysts	C 1s (C=C)	C 1s (C-O) or (C-OH)	C 1s (C=O)
Cat Ia	284.0 (74.2)	285.0 (6.5)	287.8 (19.3)
Cat Ib	284.1 (67.2)	285.3 (11.8)	287.7 (21.0)
Cat Ic	284.1 (74.6)	285.5 (6.8)	287.5 (18.6)
Cat IIa	284.0 (73.4)	285.4 (5.2)	287.4 (25.4)
Cat IIb	284.2 (69.2)	285.6 (8.8)	287.6 (22.0)
Cat IIc	284.2 (69.4)	285.7 (8.2)	287.3 (22.4)
Cat IIIa	284.3 (69.3)	285.0 (8.7)	287.3 (22.0)
Cat IIIb	284.5 (65.0)	285.4 (8.3)	287.4 (26.7)
Cat IIIc	284.5 (64.5)	285.0 (8.4)	287.6(27.1)

3.4. CYCLIC VOLTAMMETRY

Electrochemical property and performance of prepared catalysts towards methanol oxidation reaction were determined by cyclic voltammetry. Cyclic voltammograms of catalsyts were almost similar and all exhibited typical hydrogen and oxygen adsorption/desorption regions in 0.1 M $HClO_4$ solution at room temperature. 10 cycles were carried out at 50 mV/s scan rate for all catalysts with respect to saturated calomel electrode and 10^{th} cycle is shown in Figure 3.10. In case of addition of methanol to $HClO_4$ electrolyte, great change was recorded as can be seen in Figure 3.11. This change illustrates that all catalysts exhibit typical methanol oxidation reaction. Methanol electrooxidation reaction started at ~ 0.45 V reach maxima at 0.7 V in the forward scan and incompletely oxidized intermediate species such as CO started to remove from the catalyst surface at ~ 0.55 V and maximum current was observed at 0.45 V in the reverse scan.

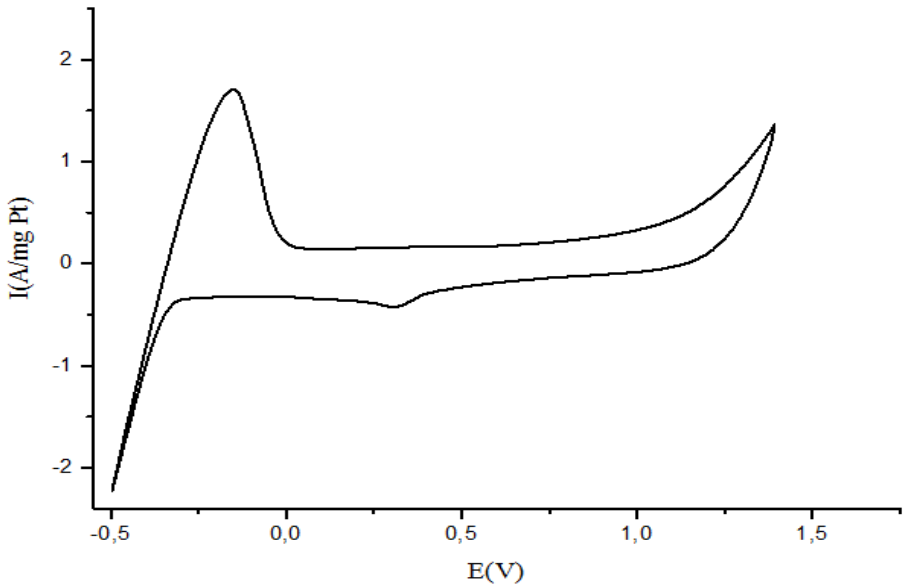

Figure 3.10. Cyclic voltammogram of catalyst Ia in 0.1 M $HClO_4$ at room temperature

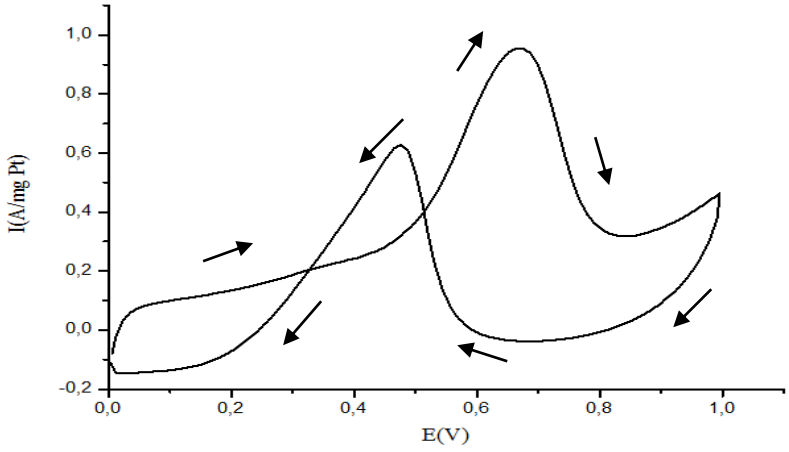

Figure 3.11. Cyclic voltammogram of catalyst Ia in 0.1 M $HClO_4$ + 0.5M CH_3OH at room temperature.

In order to observe the performance difference between the catalysts easily, cathodic part was ignored and only the anodic part of the cyclic voltammograms were considered and given in Figure 3.12 a-f. Cyclic voltammogram of catalysts were drawn by considering two parameters, one was surfactants and reducing agents, in order to observe clearly the effect of those two criteria. In the first case, the surfactants were kept constant and reducing agents were changed, Figure 3.12 a-c, and it was found that the most active catalyst was Cat III which was prepared by formaldehyde and the least active one was Cat II which was sythesized by hydrazinum hydroxide. The highest performance was observed for Cat IIIc when surfactants were kept constant as shown in Figure 3.12.f. These results indicated that reducing agents have a significant effect on the performance of the catalysts.

In the second case, the reducing agents were kept constant and surfactants were changed, Figure 3.12.d-f, and found out that the most active catalyst was Cat c which was prepared by N,N-dimethylheptanamine and the least active was Cat b was synthesized by N-methylheptanamine. Again, the highest performance was obtained for Cat IIIc in Figure 3.12.c. These results revealed that the kind of surfactants also play an important role on the performance of catalysts.

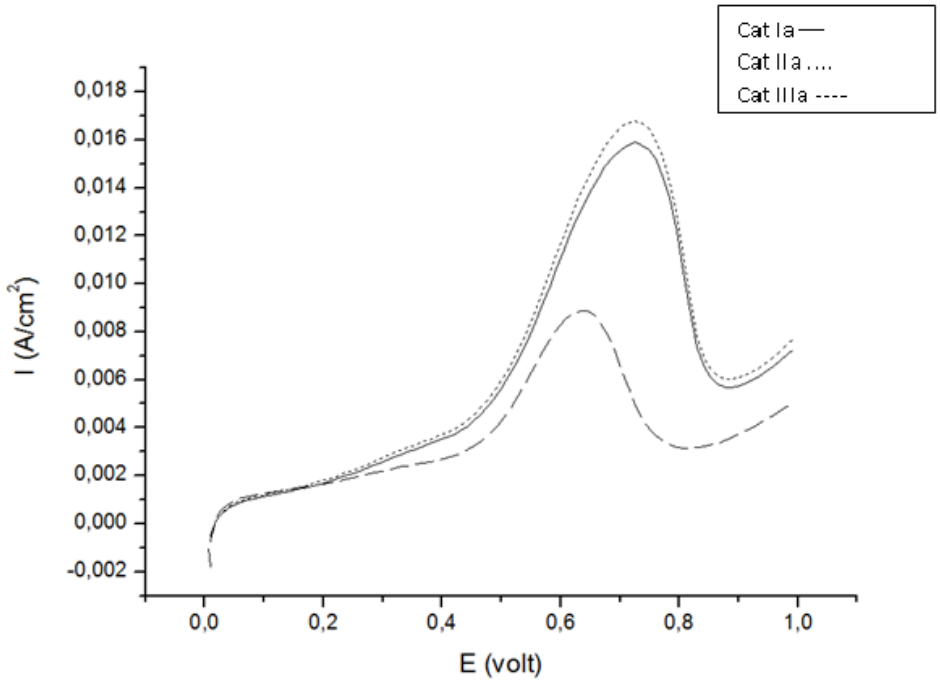

Figure 3.12.a. Cyclic voltammogram of Cat Ia (——), IIa (----), and IIIa (.....) in 0.1 M $HClO_4$ + 0.5 M CH_3OH at room temperature.

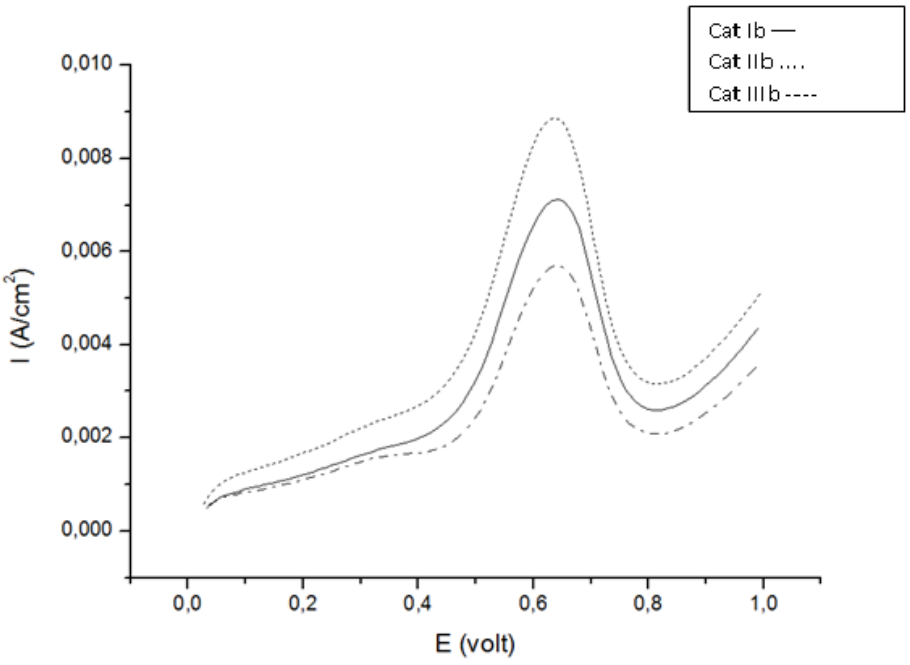

Figure 3.12.b. Cyclic voltammogram of Cat Ib (——), IIb (----), and IIIb (.....) in 0.1 M $HClO_4$ + 0.5 M CH_3OH at room temperature.

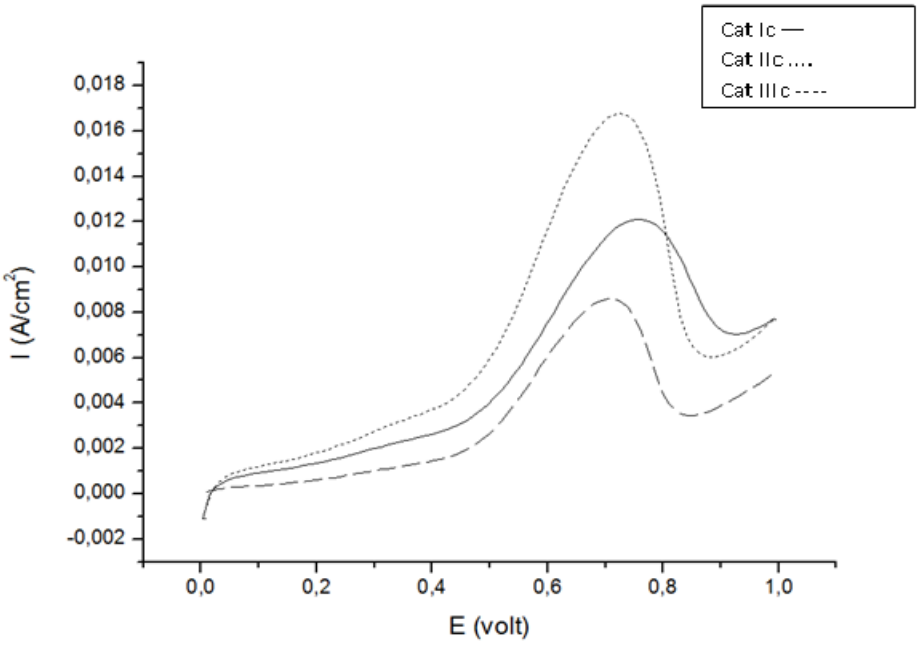

Figure 3.12.c. Cyclic voltammogram of Cat Ic (‾‾), IIc (----), and IIIc (.....) in 0.1 M $HClO_4$ + 0.5 M CH_3OH at room temperature.

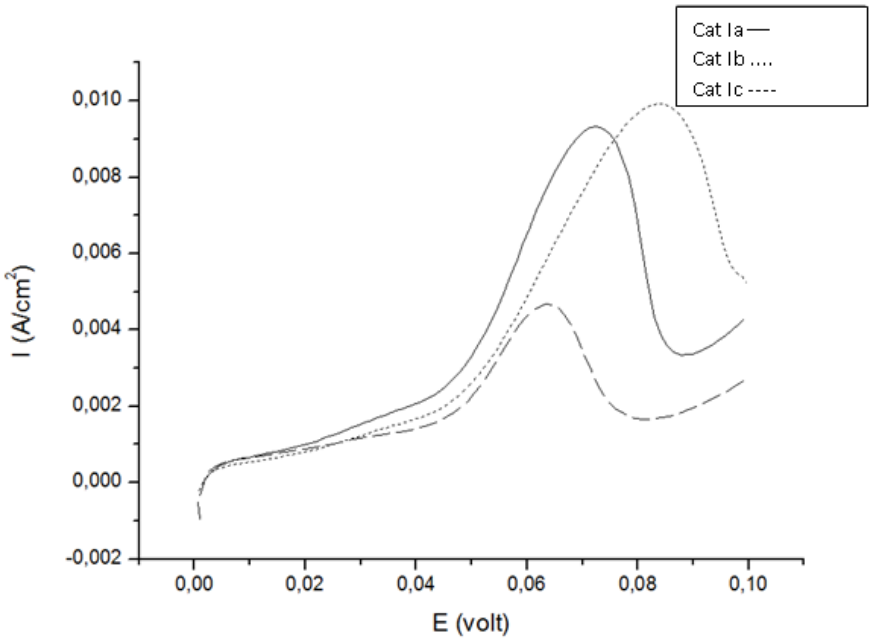

Figure 3.12.d. Cyclic voltammogram of Cat Ia (□□□ □□□ □□□ □□□ □□□), Ib (----), and Ic (.....) in 0.1 M $HClO_4$ + 0.5 M CH_3OH at room temperature.

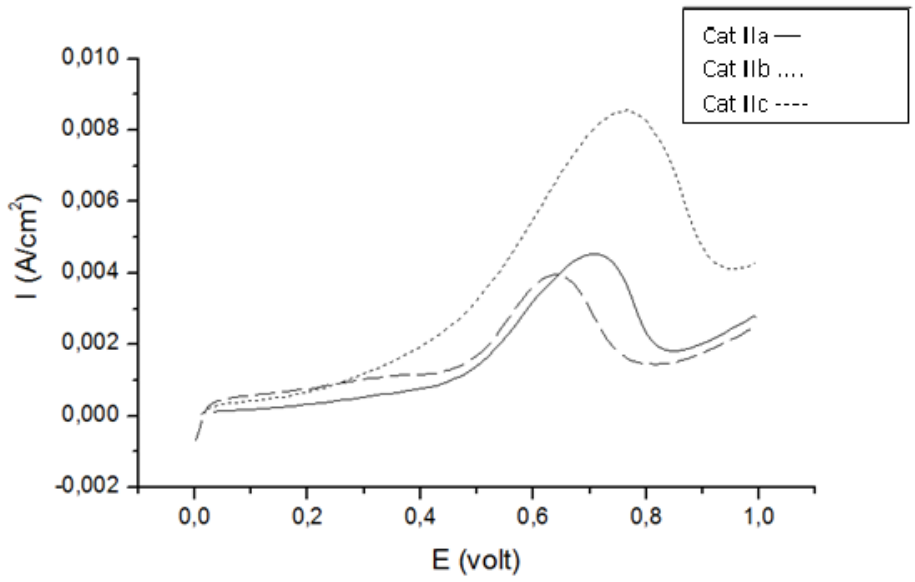

Figure 3.12.e. Cyclic voltammogram of Cat IIa (□□□ □□□ □□□ □□□ □□□), IIb (----), and IIc (.....) in 0.1 M $HClO_4$ + 0.5 M CH_3OH at room temperature.

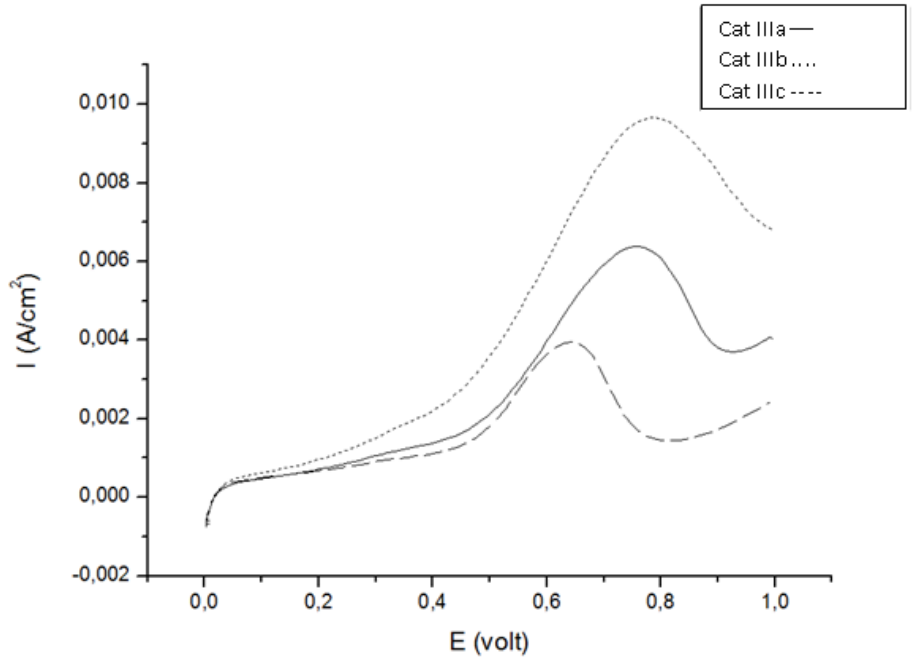

Figure 3.12.f. Cyclic voltammogram of Cat IIIa □(□□□ □□□ □□□ □□□ □□□), IIIb (----), and IIIc (.....) in 0.1 M $HClO_4$ + 0.5 M CH_3OH at room temperature.

Table 3.6. Peak potantial, maximum current and I_f/I_r ratio for all catalysts.

	Peak potential (V)	Current (A/mg Pt)	I_f/I_r
Cat Ia	0.88	0.098	1.11
Cat Ib	0.77	0.086	1.08
Cat Ic	0.79	0.096	1.19
Cat IIa	0.68	0.067	1.15
Cat IIb	0.64	0.064	1.01
Cat IIc	0.64	0.061	1.20
Cat IIIa	0.83	0.098	1.12
Cat IIIb	0.77	0.079	1.09
Cat IIIc	0.75	0.170	1.68

In addition to these, I_f/I_r ratio (I_f and I_r are the highest current density in forward scan and reverse scan, respectively) was also defined for all catalysts. It is the highest for Cat IIIc, indicating that this catalyst has the smallest poison formation on the surface of catalyst, therefore the highest performance is expected for Cat IIIc, as given above.

In order to clarify, the reason behind the performance of catalysts, chemical surface area (CSA), electrochemical surface area (ESCA), percent platinum utility (% Pt utility) and roughness factor (RF) of each catalyst have been calculated. For this purpose, CSA of platinum was determined by using following formula:

$$CSA\ (m^2/g\ Pt) = 6000 / (\rho.d)$$

where ρ is average density of Pt metal (21.4 g/cm^3) and d is the mean diameter of Pt particles in nm which was calculated from XRD and TEM data. The results are given in Table 3.7. As can be seen from the table, there is a small difference between the CSA values of catalysts, because although they are two different techniques, quite

similar results were obtained for diameter os small platinum nanoparticles which is used in the formula. The highest CSA value was obtained for Cat III, ~ 64%, and the lowest value was observed for Cat I, ~49%.

Electrochemical surface area (ECSA) of catalysts were calculated by using cyclic voltammogram and ICP results. The formula is given below:

ECSA (cm^2/g Pt) = Q / (a.b)

Where Q = Charge (mC/cm^2/Pt) calculated from hydrogen desorption region

a = Constant, 0.21 mC/cm^2/ Pt

b = Amount of platinum in g/cm^2 electrode

The average ECSA was found to be ~33.36, 23.21 and 49.38 cm^2/g Pt for Cat I, II and III, respectively, Table 3.7. It is obvious that reducing agent is an important parameter on ECSA value, but it is not possible to find the direct relationship between ECSA and the kind of surfactants. CSA and ECSA data were used to calculate percent platinum utility, Tbale 3.7., as given beow:

% Pt Utility = ECSA . 100 / CSA

The order of percent platinum utility is Cat II < Cat I < Cat III and the highest value was obtained for Cat IIIc.

Roughness factor (RF) was also calculated for each electrode and results showed the same trend ECSA values.

RF can be found by following formula:

RF= A real area / A geometrical area

A real area = Q_{hyd} (mC) / 0.21 mC/cm^2 where Q_{hyd} is the charge calculated from hydrogen desorption region

A geometrical area = Πr^2 = 0.38 cm^2, where r is the radius of electrode = 0.35 cm.

In summary, ECSA, % Pt utility and RF are important parameters on the performance of catalysts, and these parameters are the highest for Cat IIIc and it has the best performance toward methanol oxidation reaction.

Table 3.7. CSA and percent platinum utility found from TEM and XRD data, ECSA and roughness factor (RF) for all catalysts.

	CSA (m^2/gPt) (TEM) (a)	CSA (m^2/gPt) (XRD) (b)	|a-b|	ECSA (m^2/g Pt)	% Pt utility (TEM) (c)	% Pt utility (XRD) (d)	|c-d|	RF
Cat Ia	46.73	45.22	1.51	32.58	69.73	72.04	2.31	50.02
Cat Ib	50.07	47.52	2.55	31.74	63.40	66.79	3.39	49.01
Cat Ic	50.98	51.92	0.94	35.77	70.17	68.89	1.28	54.20
Cat IIa	66.76	62.31	4.45	27.90	41.80	44.78	2.98	42.32
Cat IIb	52.90	52.90	0.00	20.20	38.19	38.18	0.01	32.01
Cat IIc	52.90	56.07	3.17	21.53	40.70	38.40	2.30	32.62
Cat IIIa	62.30	58.41	3.89	48.67	78.13	83.32	5.19	73.74
Cat IIIb	66.76	68.38	1.62	47.07	70.51	68.84	1.67	72.30
Cat IIIc	63.72	62.31	1.41	52.39	82.22	84.08	1.86	78.01

CHAPTER 4

CONCLUSIONS

In this thesis, carbon supported platinum nanoparticles were prepared by using $PtCl_4$ as precursor, sodium borohydride (Cat I), hydrazinum hydroxide (Cat II) and formaldehyde (Cat III) as reducing agent and 1-heptanamine (a), N-methylheptanamine (b) and N,N-dimethylheptanamine (c) as surfactant. The following results were obtained. These are:

1. Platinum crystallizes in face centered cubic (fcc) structure for all catalysts.

2. All catalysts contain small and agglomerated particles in different shape, size and density, for instance Cat I composed of small (~5 nm) cubic and formless agglomerated (~20-150 nm) particles, Cat II involves small (~5 nm) and significant number of quite dense, spherical agglomerated (~20-300 nm) particles and Cat III includes the large number of small (~5 nm), and a few number of spherical, less dense and agglomerated (~20-200 nm) particles.

3. Platinum is found in two different oxidation state, Pt (0) and Pt (IV) with a percentage of ~64.5 - ~69.6 % for Pt (0) and ~35.5 - ~30.4 % for Pt (IV).

4. The surface of platinum is covered by adsorbed OH, H_2O, C-O, C=O, C-OH and partially crystalline carbon, and/or hydrocarbon.

5. The kind of surfactants and reducing agents affect the performance of the catalysts.

6. Electrochemical surface area (ECSA), percent platinum utility (% Pt Utility), roughness factor (RF) and I_f/I_r ratio are important criteria on the performance of catalyst.

7. The higher I_f/I_r, ECSA, % Pt utility and RF values, the better performance of catalyst.

8. Cat IIIc displayed the highest performance towards methanol oxidation reaction, indicating 2.23 times more active than commercial E-TEK catalyst.

REFERENCES

1. Atkins, P.W. (1994). Dynamic Electrochemistry, in Physical Chemistry. 5th ed. London: Oxford University Press.

2. Hill, H.A.O., Sanghera, G.S. (1990). Mediated amperometric enzyme electrodes, in Biosensors A Practical Approach (A.E.G. Cass), London: Oxford University Press.

3. Williams, D.B., Carter, C.B. (2009). Transmission Electron Microscopy: A Textbook for Materials Science. Springer, New York.

4. Muilenberg, G.E. (1979). Handbook of X-Ray Photoelectron Spectroscopy. Perkin-Elmer Corp. Minnesota.

5. Ertan, S., Şen, F., Şen, S., Gökağaç, G. (2012). Platinum nanocatalysts prepared with different surfactants for C1-C3 alcohol oxidations and their surface morphologies by AFM. Journal of Nanoparticle Research. Vol. 14. Issue 6, 1.

6. Watts, J.F. Wolstenholme, J. (2003). An Introduction to Surface Analysis by XPS and AES. John Wiley and Sons, Ltd. Chichester.

7. Nakamura, R., Ishii, K., Hashimoto, K. (2009). 121, 1634-1636. Angew. Chem. Int. Ed. 48, 1606-1608.

8. Pham, T.H., Boon, N., Aelterman, P., Clauwaert, P., De Schamphelaire, L., Vanhaecke, L., De Maeyer, K., Hçfte, M., Verstraete, W., Rabaey, K. (2008) Appl. Microbiol. Biotechnol., 77, 1119-1129.

9. Freguia, S., Masuda, M. (2009). Bioelectrochemistry, 76, 14-18.

10. Marsili, E., Baron, D.B., Shikhare, I.D., Coursolle, D., J. Gralnick, A., Bond, D.R. (2008). Proc. Natl. Acad. Sci. USA, 105, 3968- 3973.

11. Katuri, K.P., Kavanagh, P., Rengaraj, S., Leech, D. (2010). Chem. Commun. 46, 4758-4760.

12. Nielsen, L.P., Risgaard-Petersen, N., Fossing, H., Christensen, P.B., Sayama, M. (2010). Nature. 463, 1071-1074.

13. Vetter, J.K. (1961). Elektrochemische Kinetik. Springer Verlag. Berlin.

14. Cracknell, J.A., Vincent, K.A., Armstrong, F.A. (2008) Chem. Rev. 108, 2439-2461.

15. Bard, A.J., Faulkner, L.R. (2001) Electrochemical Methods. Fundamentals and Applications. Wiley.

16. Heinze, J. (1984) Angew. Chem. 96, 823-840.

17. Ertan S., Şen, F., Şen, S., Gökağaç, G. (2012). Platinum nanocatalysts prepared with different surfactants for C1-C3 alcohol oxidationz and their surface morphologies by AFM. J. Nanopart. Res. 14, 922-933.

18. Şen, F., Şen, S., Gökağaç, G. (2013). High performance Pt nanoparticles prepared by new surfactants for C1 to C3 alcohol oxidation reactions. J. Nanopart. Res. 15, 1979.

19. Kirkland, K. Chemistry: Notable Research and Discoveries, Ph.D. 2010, 139-142.

20. Bossel, U. (2000). The Birth of the Fuel Cell 1835-1845. The European Fuel Cell Forum. Switzerland.

21. Li, X. (2005). Principles of Fucel Cells. 572, 200-205. New York.

22. Öztürk, Z., Şen, F., Şen, S., Gökağaç, G. (2012). The preparation and characterization of nano-sized Pt-Pd/C catalysts and comparison of their superior catalytic activities for methanol and ethanol oxidation. Journal of Materials Science. 47, 8134-8144.

23. Wightman, R.M. (2006). Probing Cellular Chemistry in Biological Systems with Microelectrodes. Science 311 (5767): 1570 1574. doi:10.1126/science.1120027. PMID 16543451.

24. Şen, F., Şen, S., Gökağaç, G. (2011). Efficiency enhancement of methanol/ethanol oxidation reactions on Pt nanoparticles prepard using a new surfactant, 1,1-dimethyl heptanethiol. Physical Chemistry Chemical Physics. 13, 1676-1684.

25. Malvankar, N.S., Vargas, M., Nevin, K.P., Franks, A.E., Leang, C., Kim, Byoung-Chan, K., Inoue, M., Mester, S.F., Covalla, J.P., Johnson, V.M., Rotello, M.T., Tuominen, D.R. (2011). Lovley. Nat. Nanotechnol. 6, 573-579.

26. Cuenya, B.R. (2010). Thin Solid Films. 518, 3127-3150.

27. Şen, F., Şen, S., Gökağaç, G. (2011). Preparation and characterization of nano-sized Pt-Ru/C catalysts and their superior catalytic activities for methanol and ethanol oxidation. Physical Chemistry Chemical Physics. 13, 6784-6792.

28. Chung, F.H., Smith, D.K. (2000). Industrial Applications of X-Ray Diffraction. Marcel Dekker, Inc. New York.

29. Şen, F., Gökağaç, G. (2007). Different sized platinum nanoparticles supported on carbon: An XPS study on these methanol oxidation catalysts. Journal of Physical Chemistry. 111, 5715-5720.

30. Jarbad, T.B., Heineman, W.R. (1981). Patriarche. G. d. Aml. Chim. Aelo. 126.57

31. Kadirgan, F., Beyhan, S., Atilan, T. (2009). Int. J. Hydrogen Energy. 34, 4312-4320.

32. Girishkumar, G., Vinodgopal, K., Kamat, P.V. (2004). J. Phys. Chem. B, 108 (52), 19960–19966.

33. Electrochimica Acta (2002, 11 December): Vol. 48. 3, 289.

34. Gaffney, J.S., Marley, N.A. (2006). Lessons Learned from the World Trade Center Tradgedy. American Chemical Society Symposium Series 919, London:Oxford University Press. 40-65.

35. Ludwig R., Helmut K. (2008). Transmission Electron Microscopy. Edition 5.

36. Goldstein, J., Newbury, D.E., Echlin, I., Joy, D.C., Fiori, T., Lifshin, E. (1992) Scanning Electron Microscopy and X-Ray Microanalysis. Plenum Press. Edition 2.

37. Reed, S.J.B. (1996) Electron Microprobe Analysis and Scanning Electron Microscopy in Geology. Cambridge Univ. Press.

38. Goldstein, J., Newbury, D.E., Joy, D.C., Lyman, P., Echlin, E.,Lifshin, L.C., Sawyer, J.R. (2003). Scanning Electron Microscopy and X-Ray Microanalysis. Plenum Press. Edition 3.

39. Senthilnathan, J., Lin, Y.F., Rao, K.S., Yoshimura, M. (2014). Sci. Dep. 4. 4395, 1-18.

40. Yan, Y., Chisholm M.F., Duscher G., Maiti, A., Pennycook, S. J., Pantelides, S.T. (1998). Phys. Rev. Lett. 81, 3675-3678.

41. Gökağaç, G., Leger, J-M., Hahn, F. (2001). Effect of a thermal treatment on the activity of carbon-supported Pt, Pt+W and Pt+Mo electrocatalysts for methanol oxidation reaction. Zeitschrift Für Naturforschung B-Chemical Sciences. Band 56b, 1306-1314.

42. Yang, J., Lee, J.Y., Deivaraj, T.C., Too, H.P. (2004). Colloid Surface A:Physicochem. Eng. Aspects. 240, 131-134.

43. Yang, J., Deivaraj, T.C., Too, H.P., Lee, J.Y. (2004). J. Phys. Chem. B. 108, 2181-2185.

44. Nature. (1974). Vol. 250. 5463, 214-215

45. Shirley, D.A. (1972). Electron Spectroscopy. Elsevier, Amsterdam.

46. Bailey, E.C.C. (1905). Spectroscopy. Longman. Green and Co. Chapter 1. London.

47. Thompson, M., Barnes, R.M. (1992). 'Analytical Performance of Inductively Coupled Plasma–Atomic Emission Spectrometry', in Inductively Coupled Plasma in Analytical Atomic Spectrometry. Edition 2. eds. Montaser, A., Golightly, D.W. VCH Publishers. 249-297. New York.

48. Galley, P.J., Hieftje, G.M. (1994). Easily Ionizable Element (EIE) InteRFerence in Inductively Coupled Plasma Atomic Emission Spectrometry-II. Minimization of EIE Effects by Choice of Observation Volume. Spectrochim. Acta, 49B(7), 703-724.

49. Norwalk, P.E. (1990). The Guide to Techniques and Applications for Atomic Spectroscopy, CT

50. Gökağaç, G., Brendan J.K., Cshion, J.D., Brown, L.J. (1993). Characterization of carbon-supported Pt-Sn bimetallic catalysts for the electrochemical oxidation of methanol. J. Chem. Soc. Faraday Trans. 89, 151-157.

51. Lobinski, R., Adams, F.C. (1997). Speciation Analysis by Gas Chromatography with Plasma Source Spectrometric Detection. Spectrochim. Acta, 52B(13), 1865-1903

52. Hill, S.J., Bloxham, M.J., Worsfold, P.J. Chromatography Coupled with Inductively Coupled Plasma Atomic Emission Spectrometry and Inductively

Coupled Plasma Mass Spectrometry. J. Anal. At. Spectrom. 8(6), 499-515 (193).

53. Kenichi, S. Inductively coupled plasma mass spectrometer and method. US patent 6265717 B1.

54. Kollander, B., Andersson, M., Pettersson, J. (2011). Application of a fast multi element screening method using ICP-AES on different liver samples and mice organs. Journal of Trace Element in Medicine and Biology. Submitted.

55. Gökağaç, G., Kennedy, B.J., Cashion, J.D., Brown, L.J. (1993). J. Chem. Soc. Faraday Trans. 89, 151-157.

56. Rojas, S., Garcia, F.J.G., Jaras, S., Martinez-Huerta, M.V., Fierro L.G., Boutonnet, M. (2005). Applied Catalysis A: General. 285, 24-35.

57. Yonezawa, T., Toshima, N., Wakai, C., Nakahara, M., Nishinaka, M., Tominaga, T.,

Zhou, M., Xiao, P., Guo, W., Deng J., Liu, F., Zhang, Y. (2014). 161, 133-137,

58. Yonezawa, T., Toshima, N., Wakai, C., Nakahara, M., Nishinaka, M., Tominaga, T.,

Zhou, M., Xiao, P., Guo, W., Deng J., Liu, F., Zhang, Y. (2014). 161, 113-126,

59. Şen, F., Gökağaç, G. (2007). Activitiy of carbon supported platinum nanoparticles toward methanol oxidation reaction: Role of metal precursor and a new surfactant, tert-octanethiol. Journal of Physical Chemistry C. 111, 1467-1473.

60. Şen, F., Gökağaç, G. (2008). Improving catalytic efficiency in the methanol oxidation reaction by inserting Ru in face-centered cubic Pt nanoparticles

prepared by a new surfactant, tert-octanethiol. Energy & Fuels. 22, 1858-1864.

61. Gökağaç, G., Leger, J.M., Hahn, F. (2001). Z. NatuRForsch, 56 b, 1306.

62. Wang, W., Zheng, D., Du, C., Zou, Z., Zhang, X., Xia, B., Yang, H., Akins, D.L. (2007). Carbon-supported Pd-Co bimetallic nanoparticles as electrocatalysts for the oxygen reduction reaction. J. Power Sources. Vol. 167. 2, 243-249.

63. Li, X., Huang, Q., Zou, Z., Xia, B., Yang, H. (2008). Low temperature preparation of carbon-supported Pd-Co alloy electrocatalysts for methanol-tolerant oxygen reduction reaction. Electrochim. Acta, Vol. 53. 22, 6662-6667.

64. Şen, F., Gökağaç, G., Şen, S. (2013). J. Nanopart. Res.15, 1979-1988.

65. Peuckert, M.,Electrochim. Acta., 29(10), 1315-1320,.

66. Peuckert, M., Bonzel, H.P. (1984). SuRF. Sci. 145, 239-259.

67. Breiter, M. W. (1969). Electrochemical Processes in Foel Cells. Springer Verlag. Berlin.

68. Ruth, E.W. (2005) Ph.D. Research Chemist. USGS/CR/CICT.

69. Brunauer, S., Emmett, P.H., Teller, E. (1938). J. Am. Chem. Soc.60 309.

70. Gregg, S.J., Sing, K.S.W. (1982). Adsorption, Surface Area and Porosity. Academic Press. London.

71. Day, C. (2001). Colloids and Surfaces Physicochemical and Engineering Aspects. 187-188.

72. Wu, Z., Huang, X-L., Wang, Z-L., Xu, J-J., Wang, H-G., Zhang, X-B. (2014). Sci. Rep. 4, 3669, 1-20.

73. Kuanda, I., Zhu, J., Zhao, T.J., Hamner, N., Ronning, M., Raaen, S., Walmsley, J.C., Chen, D. (2010). J. Phys. Chem. C. D. Chen. J. Phys.Chem. C. 114, 1752-1762.

74. Xia, H., Zhu, D., Luo, Z., Yu, Y., Shi, X., Yuan, G., Xi, J. (2013). Sci. Rep. 3, 2978, 1-8.

75. Casella, I.G., Guascito, M.R., Sannazzaro, M.G. (1999). Electro J. Chem. 462, 202-210.

76. Luo, P.F., Kuwana, T., Paul, D.K. (1996). P.M.A. Sherwood. Anal. Chem. 68, 3330-3337.

77. Yang, S.Y. Chang, K.H., Tien, H.W, Li, Y.F., Wang, Y.S., Wang, J.Y., Ma, C.C.M., Hu, C.C. (2011). Material Chem. 21, 2374-2380.

78. Rao, K.S., Senthilnathan, J., Lin, Y.F., Yoshimura, M. (2014). Sci. Rep. 4, 4237. 1-17.

79. Tien, H.W., Hnang, Y.L., Yang, S.Y., Hsiao, S.T., Liao, W.H., Li, H.M., Wang, Y.S., Wang, J.Y., Ma, C.C.M. (2012). J. Mater. Chem. 22, 2545-2552.

80. Huang, Y., Zhai, Z., Luo, Z., Lin, Y., Liang, Z., Fang, Y. (2014). Nanotechnology. 25, 135403. 10-11.

81. Li, X., (2006). Principles of Fuel Cells, Taylor & Francis Group.

82. Şen, S., (2008). Activity of Carbon Supported Platinum Nanoparticles Toward Methanol Oxidation Reactions: Role of Metal Precursor and New Surfactants, Master of Science Thesis in Chemistry, METU, Ankara.

83. Şen, F.,(2012). The Preparation and Analysis of New Carbon Supported Pt and Pt+Second Metal Nanoparticles Catalysts for Direct Methanol Fuel Cells, Doctor of Philosophy Thesis in Chemistry, METU, Ankara.